ELSEVIER

Contents lists available at ScienceDirect

# Climate Services

journal homepage: www.elsevier.com/locate/cliser



Original research article

# Unveiling heatwave events in Bangladesh: Insights from observational records and ERA5 reanalysis data

Salit Chakma <sup>a</sup>, Abu Yousuf Md Abdullah <sup>b</sup>, Mohammed Sarfaraz Gani Adnan <sup>c,\*</sup>, Md Saqib Shahriar <sup>d</sup>, Mohammad Al Masum Molla <sup>e</sup>, Quazi K. Hassan <sup>f</sup>, Ashraf Dewan <sup>g</sup>

- a Department of Population Health Science, University of Mississippi Medical Center, 2500 North State Street, Jackson, MS 39216, United States
- <sup>b</sup> School of Planning, University of Waterloo, ON, Canada
- <sup>c</sup> Department of Civil and Environmental Engineering, Brunel University of London, Uxbridge UB8 3PH, United Kingdom
- d Center for Environmental and Geographic Information Services (CEGIS), House-6, Road 23/C (16/A), Gulshan 1, Dhaka 1212, Bangladesh
- e Gaylord College of Journalism and Mass Communication, University of Oklahoma, United States
- f Department of Geomatics Engineering, University of Calgary, 2500 University Drive NW, Calgary Alberta T2N 1N4, Canada
- g Spatial Sciences Discipline, School of Earth and Planetary Sciences, Curtin University, Perth 6102, Australia

#### ARTICLE INFO

Keywords:
Bangladesh
Heat index
Heatwave characteristics
Heatwave indices
Observational data
ERA5

#### ABSTRACT

Heatwaves (HWs) are escalating in frequency and intensity, posing serious risks to human health, agriculture, and infrastructure worldwide. However, the lack of a universally accepted definition of HWs complicates consistent characterization across regions. In Bangladesh, a subtropical country increasingly vulnerable to extreme heat, the dynamics of HWs remain insufficiently understood. This study aims to bridge that knowledge gap by analyzing three decades of observational data to characterize HWs in Bangladesh, using ambient and apparent temperature metrics. Five HW indices were employed to assess 24-hour (EHF), daytime (CTX90pct, TX90), and nocturnal (CTN90pct, TN90) HW patterns, with humidity effects incorporated through apparent temperature-based indices. HWs were defined as events lasting at least three consecutive days, reflecting the heightened health risks of prolonged exposure. HWs were evaluated in terms of frequency, duration, intensity, and early onset patterns. Station-based observations were compared against corresponding estimates derived from ERA5 reanalysis data. The  $90^{th}$  percentile of daily temperature emerged as a robust operational threshold for HW characterization in Bangladesh. Declines in temperature variability during HW events were linked to reduced intensities for indices sensitive to short-term variability or independent of seasonality. Humidity exerted a stronger influence on nocturnal HWs than on daytime events, while seasonal variations in temperature and humidity during the pre- and post-monsoon periods significantly shaped HW characteristics. These findings provide new insights into the spatiotemporal dynamics of HWs in Bangladesh, offering an evidence base to inform adaptation strategies in other subtropical regions facing similar climate threats.

Practical implications: This study provides critical insights into the growing challenges of HWs in Bangladesh, highlighting their increasing frequency, duration, intensity, and earlier onset. The findings underscore the importance of adopting the 90<sup>th</sup> percentile of daily temperature as a reliable threshold for HW characterization, tailored to Bangladesh's subtropical climate. The study reveals distinct regional and seasonal patterns, with coastal areas experiencing prolonged HWs and humidity-driven nocturnal events, which significantly disrupt nighttime recovery and productivity. Policymakers can leverage these insights to develop localized mitigation strategies, such as early warning systems, urban heat management plans, and infrastructure adaptations to reduce HW impacts. The results emphasize the role of humidity in intensifying heat stress, calling for integrated approaches that consider both ambient temperature and apparent temperature metrics in HW assessments. Furthermore, the methodology used in this study is transferable to other similar climatic contexts, making the results valuable for informing policy in regions beyond Bangladesh that face comparable challenges. By addressing gaps in observational data and incorporating indoor heat stress and continuous surface data in future research, the findings offer a pathway to designing more robust climate resilience frameworks. These measures

E-mail address: sarfaraz.adnan@brunel.ac.uk (M.S.G. Adnan).

<sup>\*</sup> Corresponding author at: Mohammed Sarfaraz Gani Adnan, Department of Civil and Environmental Engineering, Brunel University of London, Uxbridge UB8 3PH, United Kingdom.

are essential for safeguarding vulnerable populations, ensuring public health, and minimizing socio-economic losses from extreme heat events both locally and globally.

#### 1. Introduction

Heatwaves (HWs) have emerged as a pressing global issue due to their profound impacts on agriculture (Miralles et al., 2019; Miller et al., 2021), ecosystems (Handmer et al., 2012; Li and Amatus, 2020), human health (Dong et al., 2021; Ebi et al., 2021), labor efficiency (Yin et al., 2020), and productivity (García-León et al., 2021; Zhao et al., 2021). The increasing frequency and intensity of HWs are strongly linked to anthropogenic climate change, with projections suggesting even greater severity and recurrence in the future (Jyoteeshkumar reddy, Perkins-Kirkpatrick and Sharples, 2021; Kornhuber et al., 2024).

HWs were ranked as the 6<sup>th</sup> and 7<sup>th</sup> most destructive natural disasters globally during the first two decades of the 21<sup>st</sup> century (CRED and UNDRR, 2020), during which there was a significant rise in the extent of landmass experiencing extreme heat (Vogel et al., 2019). Extreme heat events have led to substantial loss of life, accounting for 91 % of the total natural hazards-related deaths between 2000 and 2019 (CRED and UNDRR, 2020). In Europe, for instance, catastrophic HWs in 2003 and 2010 led to over 72,000 and 55,000 fatalities, respectively (Habeeb, Vargo and Stone, 2015; CRED and UNDRR, 2020). In South Asia, the 2018 HWs in India severely impacted agrarian communities, causing substantial damage to agricultural productivity (Vogel et al., 2019).

Bangladesh, as one of the most densely populated countries in the world, is highly vulnerable to HWs (Kagawa, 2022), ranking second globally in terms of human exposure to heat (Tuholske et al., 2021). Prolonged HW episodes in Bangladesh from 2022 to 2024 have resulted in significant health, infrastructural, and socio-economic challenges (Mohammad and Weng, 2024). Various reports highlight increases in morbidity (Mustajib, 2024) and mortality (Hossain and Manik, 2022), elevated energy demands with frequent power outages (Mahmud, 2023; Paul and Varadhan, 2023), and damage to critical infrastructure such as roads (Adhikary, 2024) and railways (Chowdhury, 2024) during HWs. Other consequences include disruptions to education (Ng, 2024) and severe water shortages (Nandy, 2024). The economic toll of heat stress in Bangladesh is substantial, with an estimated annual per capita loss of \$281 (Bardhan et al., 2024).

Climate data from 2022 revealed July and August as having the highest average monthly temperatures and lowest rainfall since 1989. The capital, Dhaka, experienced a maximum temperature of 40.4 °C in April 2022 (Majumder, 2024) and recorded the highest temperature of 40.6 °C since 1960 during the April 2023 HW (Zachariah et al., 2023). April 2024 was documented as the hottest April on record (The Economic Times, 2024), affecting over three-quarters of the country and lasting for more than 25 consecutive days, the longest HW episode since 1948 (Islam, 2024). Between April 15, 2023, and April 15, 2024, 57 days of extreme heat events were reported, which would have been four times shorter without anthropogenic-influenced climate change (Nabil, 2024). These extreme heat events are exacerbated by anthropogenic activities that have contributed to a 2 °C rise in the heat index (HI) since 1950 (Zachariah et al., 2023). The mean temperature of Bangladesh has also increased by 0.5 °C between 1976 and 2019 and is projected to rise by 2.4 °C by 2100 (Mahmud et al., 2021).

Despite the growing severity of HWs, research on their dynamics and impacts in Bangladesh remains limited due to sparse observational data (Alexander et al., 2006) and the lack of localized models for accurate predictions (Nissan et al., 2017). Existing studies in Bangladesh often focus on surface urban heat islands (SUHI) (Dewan et al., 2021) or specific aspects of extreme heat episodes, such as extreme temperature events (Abdullah et al., 2022), HW vulnerabilities (Adnan et al., 2024), heat exposure (Yasumoto et al., 2019), and health impacts of heat stress (Wu et al., 2018). However, most of these studies rely on remotely

sensed data, either as a proxy or as dry bulb temperature, overlooking the combined effects of dry bulb air temperature and humidity, which are critical in humid climatic regions (Mohammad and Weng, 2024). Although humidity is essential to the understanding of HW impacts on humans, as it significantly influences apparent heat stress, particularly during extreme heat events (Fischer and Schär, 2010; Guo et al., 2024), it remains inadequately addressed in HW definitions for Bangladesh. The only exception is Nissan et al. (2017), who developed a public health-focused HW definition using a regression model to link mortality with HW variations.

Furthermore, past studies (Rahman et al., 2024) and the Bangladesh Meteorological Department (BMD) predominantly rely on absolute threshold measures (such as > 36 °C) for HW detection (Bangladesh Red Crescent Society, 2021). While absolute thresholds are straightforward and easy to interpret, they have significant limitations, including failure to account for acclimatization, temperature variability, and seasonal changes (Barriopedro et al., 2023). Studies using relative thresholds have typically employed the 95<sup>th</sup> percentile of daily temperature to define HWs in Bangladesh, without adequately assessing the suitability of alternative percentiles, such as the 90<sup>th</sup> or 99<sup>th</sup> (Nissan et al., 2017; Wu et al., 2018). Moreover, as regional warming intensifies, the relevance of relative thresholds may diminish, particularly in dry atmospheric conditions that could exacerbate future extreme events. Additionally, there is a notable gap in the literature addressing nocturnal HWs, which are critical in evaluating the impact of heat stress during nighttime recovery periods.

Given these gaps, a comprehensive study on HWs in Bangladesh is essential, focusing on their characteristics, seasonality, and spatial distribution using *in-situ* observational data. Leveraging available observational records, this study aims to: (1) identify an appropriate percentile temperature threshold for defining HWs; (2) evaluate HW indices to characterize 24-hour, daytime, and nocturnal HWs, assessing their frequency, duration, intensity, and early onset; and (3) analyze the spatiotemporal distribution and trends of HWs across Bangladesh.

# 2. Materials and methods

# 2.1. Study area

Bangladesh is a densely populated South Asian country that faces significant developmental challenges due to its unique geographical, topographical, and climatic conditions. The country experiences a monsoon-driven climate system, characterized by four distinct meteorological seasons: a relatively dry and warm pre-monsoon (March–May), a humid monsoon (June–September), a transitional post-monsoon (October–November), and a dry, cool winter (December–February). The humid monsoon season contributes over 70 % of the country's annual rainfall, while the pre-monsoon and post-monsoon periods are marked by high temperature variability.

The country is highly susceptible to climate extremes, including HWs, due to its dense population and limited adaptive capacity (Khan et al., 2019). Its proximity to the Bay of Bengal significantly influences its climatic patterns (Shetye et al., 1996), as the southerly and southwesterly monsoon flows transport warm, humid air inland during summer (Ehsan et al., 2023), increasing humidity and predisposing the region to HWs and heat stress (Choi et al., 2021). Major metropolitan areas, such as Dhaka, Chittagong, Khulna, Rajshahi, and Sylhet, are particularly vulnerable to HWs. Factors contributing to this vulnerability include elevated surface temperatures, rapid urbanization, an increasing proportion of built-up areas, limited green spaces, and the poor socioeconomic status of many residents (Adnan et al., 2024). These

conditions exacerbate the impacts of HWs, making the need for localized studies and adaptive measures increasingly urgent.

#### 2.2. Data

This study utilized weather data from the BMD spanning a 30-year period (1993–2022). Data were obtained from 33 meteorological stations, selected based on their availability and geographic distribution to provide comprehensive national coverage (Fig. 1). Daily dry bulb air temperature and average relative humidity (RH) data were collected. For clarity, dry bulb air temperature is referred to as air temperature ( $T_{\rm air}$ ) and includes minimum ( $T_{\rm min}$ ) and maximum temperatures ( $T_{\rm max}$ ).

To address missing data, the study employed Multiple Imputation by Chained Equations (MICE), a robust statistical technique that imputes missing values by generating multiple plausible estimates based on existing data (Zhang, 2016). This method constructs a prediction model to fill gaps using seasonal and monthly patterns, ensuring that the imputed values align with observed records (Abdullah et al., 2022). A total of 30 imputed datasets were created using a Bayesian framework and the predictive mean matching algorithm, which helps preserve data integrity and variability (van Buuren, 2018). This gap-filling approach ensured that missing values did not significantly bias the analysis or compromise the quality of the results.

#### 2.3. Methods

The methodology employed in this study is divided into two parts (Fig. 2). First, the identification of HWs, which was carried out based on (i) ambient and (ii) apparent temperatures. Here,  $T_{\rm air}$  was used as the ambient temperature, while HI was used as the apparent temperature

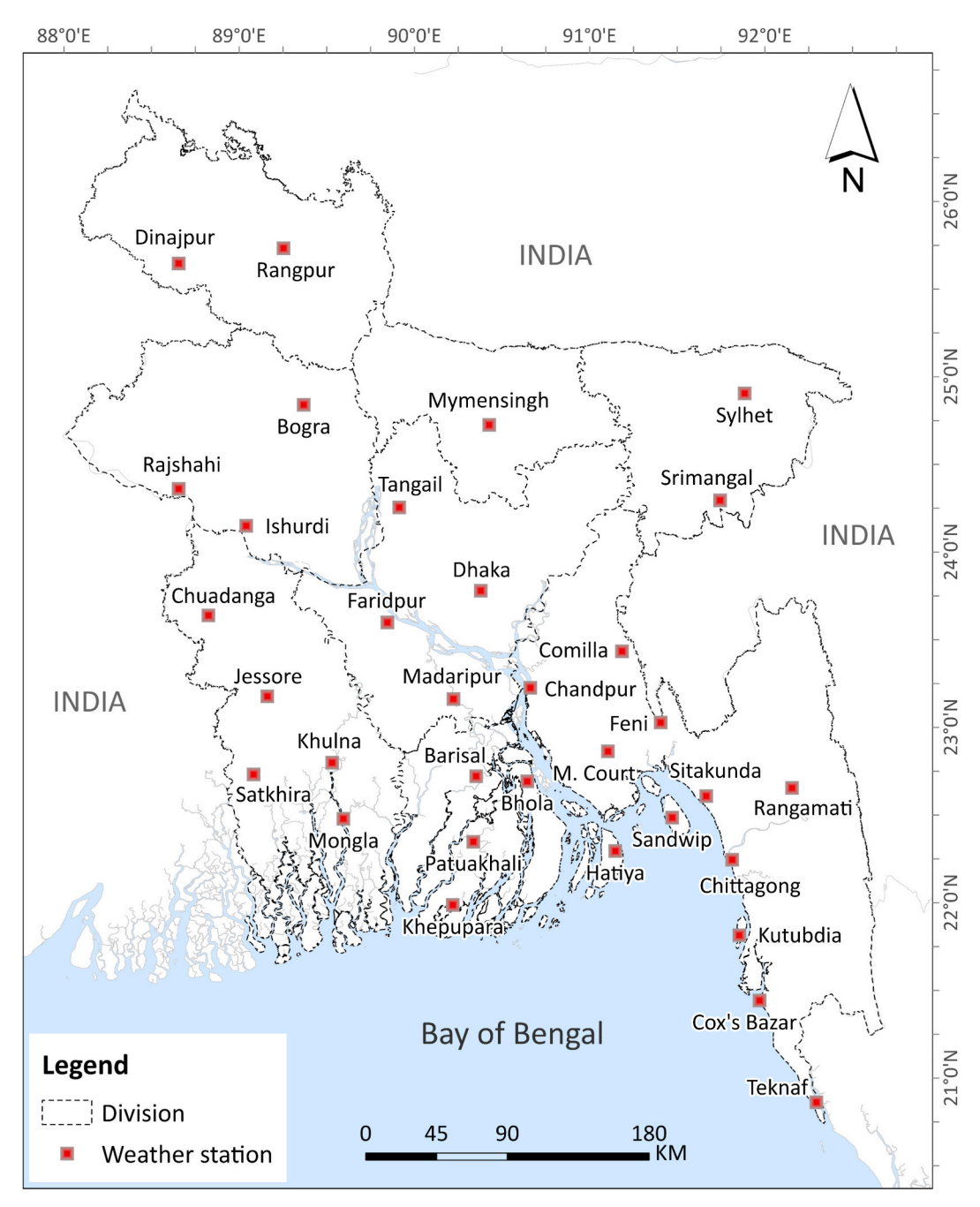


Fig. 1. Spatial distribution of the 33 weather stations considered in this study.

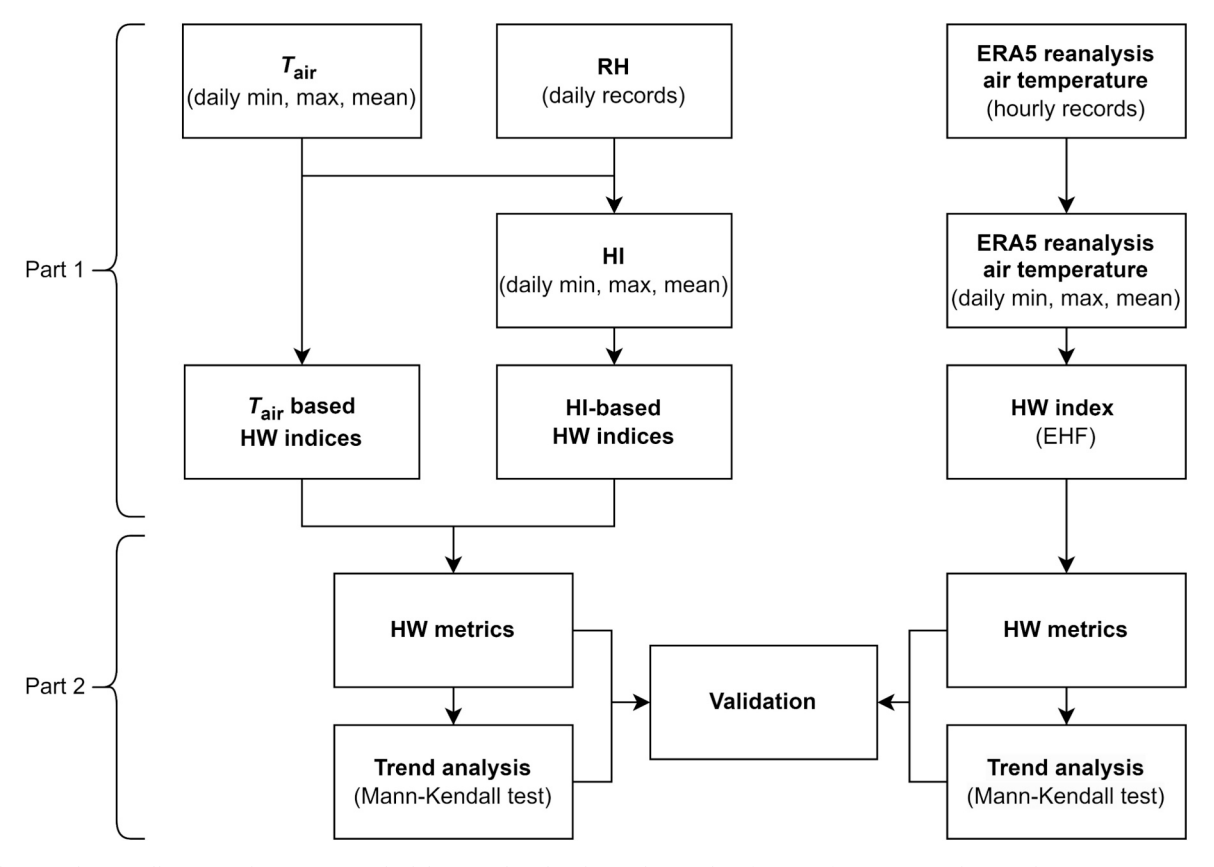


Fig. 2. Schematic diagram illustrating the two-part methodology employed in this study: (1) identification of HWs using ambient and apparent temperatures and (2) analysis of HW characteristics, including frequency, duration, intensity, and onset trends.

(Fischer and Schär, 2010). Five HW indices—Excess Heat Factor (EHF), CTN90pct, CTX90pct, TN90, and TX90—were used to identify HWs based on both ambient and apparent temperatures.

Heat events defined using HI are referred to as humid heat events, accounting for heat stress induced by humidity, which is reportedly frequent in Bangladesh (Zachariah et al., 2023). The same five indices noted earlier were calculated using HI to define HWs under humid conditions and were denoted with a suffix "-HI" (e.g., EHF-HI, CTN90pct-HI, CTX90pct-HI, TN90-HI, and TX90-HI). A threshold of three consecutive days was employed for all HW indices, meaning that a high temperature persisting for at least three consecutive days was

considered a HW event.  $T_{\rm air}$  and RH records for the winter months (December–February) were excluded from the analysis, as these months are uncommon for exhibiting heat-related stress.

Second, six metrics were adopted to ascertain HW characteristics, including frequency (HWN), duration (HWD, HWF), intensity (HWM, HWA), and onset (HWT) of the events. The onset was calculated by counting the number of days from March 1 (similar to the day of the year) for each year. Trend analysis of these HW characteristics was performed with the non-parametric Mann-Kendall test (Mann, 1945) in conjunction with Sen's slope estimator (Sen, 1968). Increasing or decreasing trends in the onset indicated early or delayed HWs.

Table 1

HW indices and their calculation methods. All indices define a HW event as a period of at least three consecutive days meeting the specified criteria.

Index	Туре	Input	Calculation method	Characteristics	Corresponding HW index for humid condition*
EHF	Composite index from average temperature	Average $T_{\rm air}$	EHF = EHI <sub>sig</sub> × max(1, EHI <sub>accl</sub> ) EHI <sub>sig</sub> = 3-day average $T_{air}$ – $90^{th}$ or $95^{th}$ percential of climate normal EHI <sub>sig</sub> = 3-day average $T_{air}$ – $90^{th}$ or $95^{th}$ percentile of climate normal EHI <sub>accl</sub> = 3-day average $T_{air}$ – preceding 30-day average $T_{air}$	Detects HWs based on average temperature and accounts for deviation from climatological percentile ( <i>EHI</i> <sub>sig</sub> ) and acclimatization ( <i>EHI</i> <sub>accl</sub> )	ЕНГ-НІ
CTN90pct	Nocturnal HW index	$T_{\min}$	$T_{\rm min} > 90^{ m th}$ percentile of 15-day moving window (15-day $ imes 30$ years = 450 values for each day)	Detects nighttime HWs accounting for seasonality	CTN90pct-HI
CTX90pct	Daytime HW index	$T_{\rm max}$	$T_{\rm max} > 90^{\rm th}$ percentile of 15-day moving window (same as CTN90pct)	Same as CTN90pct but for daytime HWs	CTX90pct-HI
TN90	Nocturnal HW index	$T_{ m min}$	$T_{\rm min} > 90^{ m th}$ percentile of climate normal	Detects nocturnal HWs exceeding climatological percentile thresholds for consecutive ≥ 3 days	TN90-HI
TX90	Daytime HW index	$T_{\text{max}}$	$T_{\rm max} > 90^{\rm th}$ percentile of climate normal	Same as TN90 but for daytime HWs	TX90-HI

<sup>\*</sup> For HW indices that incorporate humidity, the input variable is HI—such as daily average, minimum, maximum HI—rather than  $T_{\rm air}$ . All other aspects of the calculation method remain the same as their corresponding  $T_{\rm air}$ -based indices.

# 2.3.1. Identification of HWs from ambient and apparent temperatures i) Ambient temperature-based HWs

HWs defined by ambient temperature were derived through the direct use of  $T_{air}$  in constructing the indices listed in Table 1.

EHF: The EHF (Nairn et al., 2009) is a quantitative metric used to denote potential HW events by examining the deviation of the current 3day average temperature from both climatological normal (1993–2022) and the preceding 30 days' average temperature. The deviation from the climatological normal provides a significance index (EHI<sub>sig</sub>), while the deviation from the preceding 30 days' average temperature yields an acclimatization index (EHI<sub>accl</sub>). EHI<sub>sig</sub> uses an upper percentile figure, typically the 90<sup>th</sup> (Oliveira et al., 2022; Piticar, et al., 2018) or 95<sup>th</sup> percentiles (Nairn et al., 2009; Tolika, 2019), from daily records over a multi-decadal period to establish a reference value for the normal or climate baseline.  $EHI_{accl}$  is particularly important from a human health perspective, as its positive values indicate a sudden temperature change to which humans may fail to acclimatize (Tolika, 2019). Both indices measure temperature anomalies and are expressed in degrees Celsius, providing insights into the severity of HWs and the associated risks they pose to human and environmental systems (Nairn and Fawcett, 2014). The EHF is a product of EHIsig and EHIaccl (for more details, please see Nairn et al. (2009)).

CTN90pct and CTX90pct: Two indices, CTN90pct and CTX90pct (Perkins and Alexander, 2013), were used to determine nocturnal and daytime HWs, respectively. CTN90pct relies on the percentile threshold of  $T_{\rm min}$  from a 15-day moving window, while CTX90pct depends on the percentile threshold of  $T_{\rm max}$  from the same 15-day moving window. These moving windows around calendar days result in different percentile thresholds for each calendar day, accounting for seasonality (Perkins and Alexander, 2013). For 30 years of data used, percentile thresholds for each calendar day were calculated from 150 (15  $\times$  30) daily records (Zhang et al., 2005; Fischer and Schär, 2010).

While the adverse health impacts of extreme daytime heat are well-documented, recent studies have highlighted the growing risks of nighttime heat (Wu et al., 2023). This study included nocturnal HWs in the analysis, as limited research has explored their mechanisms (Luo et al., 2022; Thomas, et al., 2020), particularly in the context of Bangladesh.

**TN90 and TX90:** The likelihood of extremely high temperatures increases in regions that frequently surpass historical temperature records (Yin et al., 2020). Therefore, this study used climatological percentile thresholds to define nocturnal and daytime HWs using TN90 and TX90 indices for comparison with historical records. For TN90, any hot spell exceeding the percentile threshold, calculated from the daily  $T_{\rm min}$  of 30 years, was registered as an HW event. TX90 was calculated using the same methodology, but  $T_{\rm max}$  values were used.

# ii) Apparent (perceived) temperature-based HWs

**HI:** The HI evaluates apparent or human-perceived temperature, representing heat stress felt in shaded conditions (Steadman, 1979). It was calculated by combining  $T_{\rm air}$  with RH (Fischer and Schär, 2010), following the National Oceanic and Atmospheric Administration (NOAA) guidelines (https://www.wpc.ncep.noaa.gov/html/heatindex\_equation.shtml).

HWs from HI: The subtropical climate of Bangladesh necessitates considering both air temperature and humidity to accurately assess heat stress in humid conditions. Accordingly, daily average, minimum, and maximum HI values were incorporated into the HW indices, denoted as EHF-HI, CTN90pct-HI, CTX90pct-HI, TN90-HI, and TX90-HI. The methodologies for estimating these indices mirror those of their ambient temperature counterparts (EHF, CTN90pct, CTX90pct, TN90, and TX90), with the only difference being the use of HI as the input parameter.

#### 2.3.2. Characterizing HWs

To characterize HW events, six HW metrics (Perkins and Alexander, 2013) were calculated (Table 2). These metrics were summarized on a

Table 2
HW metrics used for characterizing HW events.

HW metric	Characteristics	Unit
HW number (HWN)	The frequency of HW events.	Event
HW duration (HWD)	The number of days for the longest HW event.	day
HW frequency sum (HWF)	The sum of all frequencies of HW days.	day
HW magnitude (HWM)	Average intensity of HWs.	°C <sup>2</sup> for only
	Calculated based on anomaly from the threshold.	EHF and EHF- HI
HW amplitude	The maximum intensity of HWs or the	
(HWA)	intensity of the hottest HW event.	°C for all other indices
	Calculated based on anomaly from the threshold.	
HW timing (HWT)	First HW event's timing or onset.	Day of the year
	Considered from the first annual day of a	
	specific time/season, revealing onset	
	pattern. In this study, HWT is relative to	
	March 1 for a year is considered.	

monthly, seasonal, and annual basis, as well as for the entire study period (1993–2023) for each ground station. The spatial distribution of the metrics was evaluated by computing the mean over the entire study period, while the temporal distribution was reported as monthly, seasonal, and annual summaries.

#### 2.3.3. Trend detection

The statistical significance of the trends was assessed using the Mann-Kendall test, available in the pyMannKendall Python package (Hussain and Mahmud, 2019). The Mann-Kendall test is a non-parametric method that tests for the presence of a monotonic trend, considering the rank correlation of observations. In addition, the magnitude of the monotonic trend was determined using Sen's slope (Sen, 1968). The non-parametric Sen slope estimator was applied to identify temporal trends in the HW metrics.

# 2.3.4. Validation with ERA5 reanalysis data

To validate the results from observational  $T_{\rm air}$ , ERA5 reanalysis data for 2-m  $T_{\rm air}$  was used (Hersbach et al., 2020). Hourly ERA5 reanalysis data covering all of Bangladesh was obtained from the Copernicus Climate Data Store (Copernicus Climate Data Store, 2018). Daily  $T_{\rm max}$  and  $T_{\rm min}$  temperatures were resampled from the hourly data using the xarray Python package (Hoyer et al., 2023). The Python tool ehfheatwaves (Loughran, 2021) was used to retrieve daily EHF scores. When applied to ERA5 reanalysis data, the tool generates three outputs:

- i) EHF: EHF scores for each day.
- ii) *events*: Binary values indicating whether the EHF score exceeded zero, signifying a HW event.
- ends: The duration of HW events, starting from their date of onset.

Using the retrieved *EHF* and *ends* variables from the *ehfheatwaves* tool, six HW metrics were calculated (Table 2). Pearson's correlation was used to calculate the correlation coefficients between the ERA5 reanalysis data and the station-observed metrics.

# 3. Results

# 3.1. Heatwave events

The findings of this study revealed a distinct difference between the two HW thresholds (e.g.,  $90^{th}$  and  $95^{th}$  percentiles) in identifying HW

events, regardless of whether  $T_{\rm air}$  or HI-based indices were used. A comparison of linear trends and interannual variations of the metrics derived from  $T_{\rm air}$  (Fig. 3) and HI (Fig. S1, supplementary document) indicated that the 90<sup>th</sup> percentile was more suitable for capturing the frequency of HW events across the country. HW indices based on the 90<sup>th</sup> percentile consistently detected a considerable number of measurable events.

In contrast, the 95<sup>th</sup> percentile threshold failed to clearly identify HW events when acclimatization and seasonal cycles were considered, particularly with HI-based indices (Fig. S1(a), supplementary document). For instance, no HW events were detected in 2007 using the CTX90pct-HI index, and in 1993 and 2018 using the CTN90pct-HI index. Additionally, the CTX90pct-HI and TX90-HI indices identified only one HW event per year. Metrics related to intensity (HWM and HWA) and onset (HWT) were not effective in determining the most appropriate percentile thresholds, as they exhibited identical interannual variations

and linear trends (see Fig. 3(d-f) and Supplementary Fig. S1(d-f)).

# 3.1.1. Monthly and seasonal distribution of HWs

Fig. 4 and Fig. 5 exhibit the monthly distribution of HW events and HW days derived from various indices. Both figures demonstrate similar patterns and distributions; however, the total HW days (Fig. 5) show greater variability compared to the total HW events (Fig. 4). This variability highlights disparities in the number of HW events and days across different regions of Bangladesh. The monthly distribution of total HW events and days suggests an earlier onset of  $T_{\rm air}$  –based HWs compared to HI-based HWs. This distinction is particularly evident in indices such as EHF, TN90, TX90, and their HI-based counterparts. Notably, the HI-based CTN90pct and CTX90pct indices indicate an increased number of HW events (Fig. 4(d-f)) and HW days (Fig. 5(d-f)) in November, reflecting a significant percentage of events occurring during the postmonsoon months (Fig. 6).

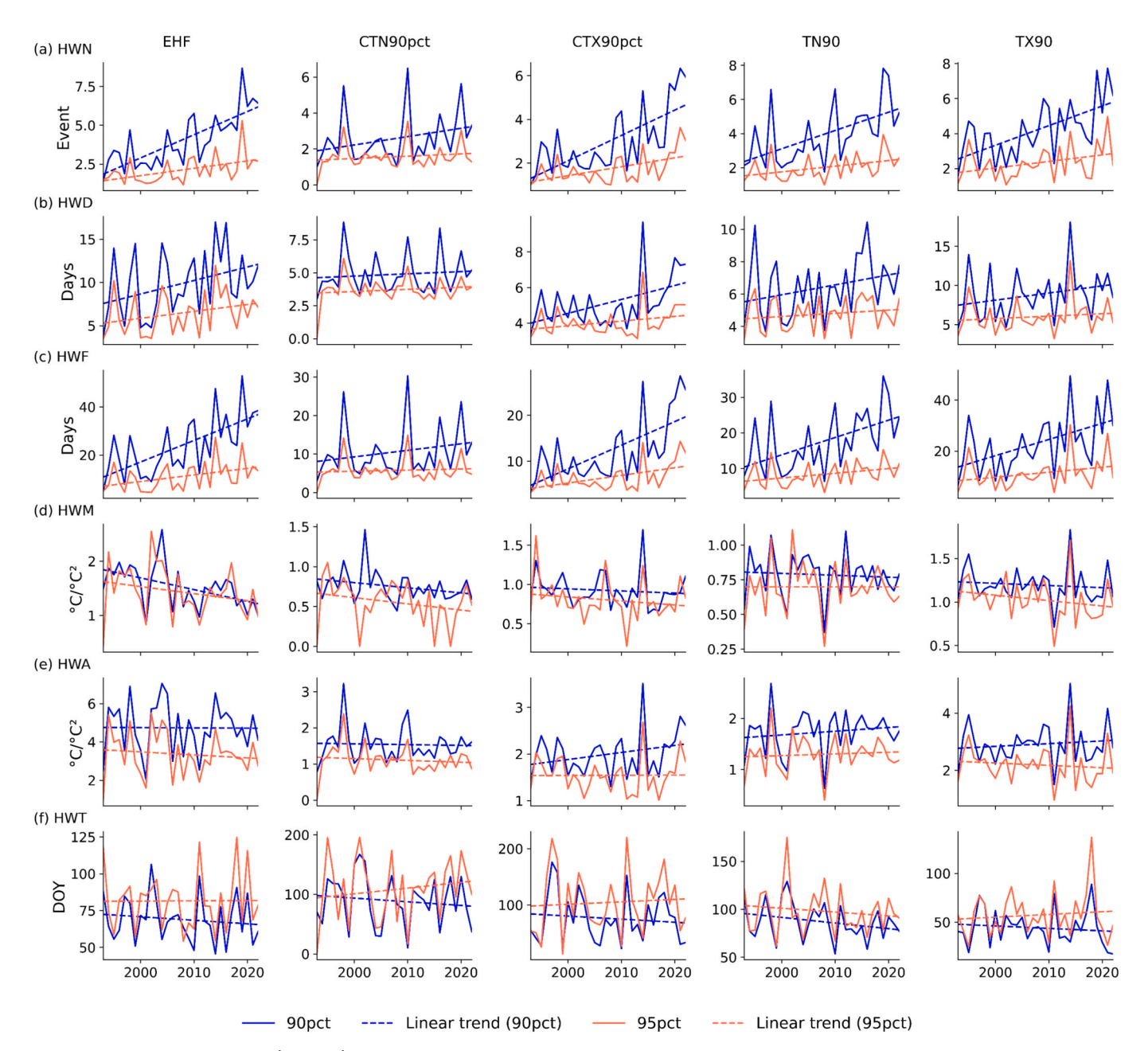


**Fig. 3.** HW metrics derived from  $90^{\text{th}}$  and  $95^{\text{th}}$  percentiles of  $T_{\text{air}}$ . CTN90pt and CTX90pct used a 15-day window of daily  $T_{\text{min}}$  and  $T_{\text{max}}$  across the study period (1993–2022), accounting for seasonality, while TN90 and TX90 indices used climatological percentile thresholds. The HW metrics are: (a) HWN, (b) HWD, (c) HWF, (d) HWM, (e) HWA, and (f) HWT.

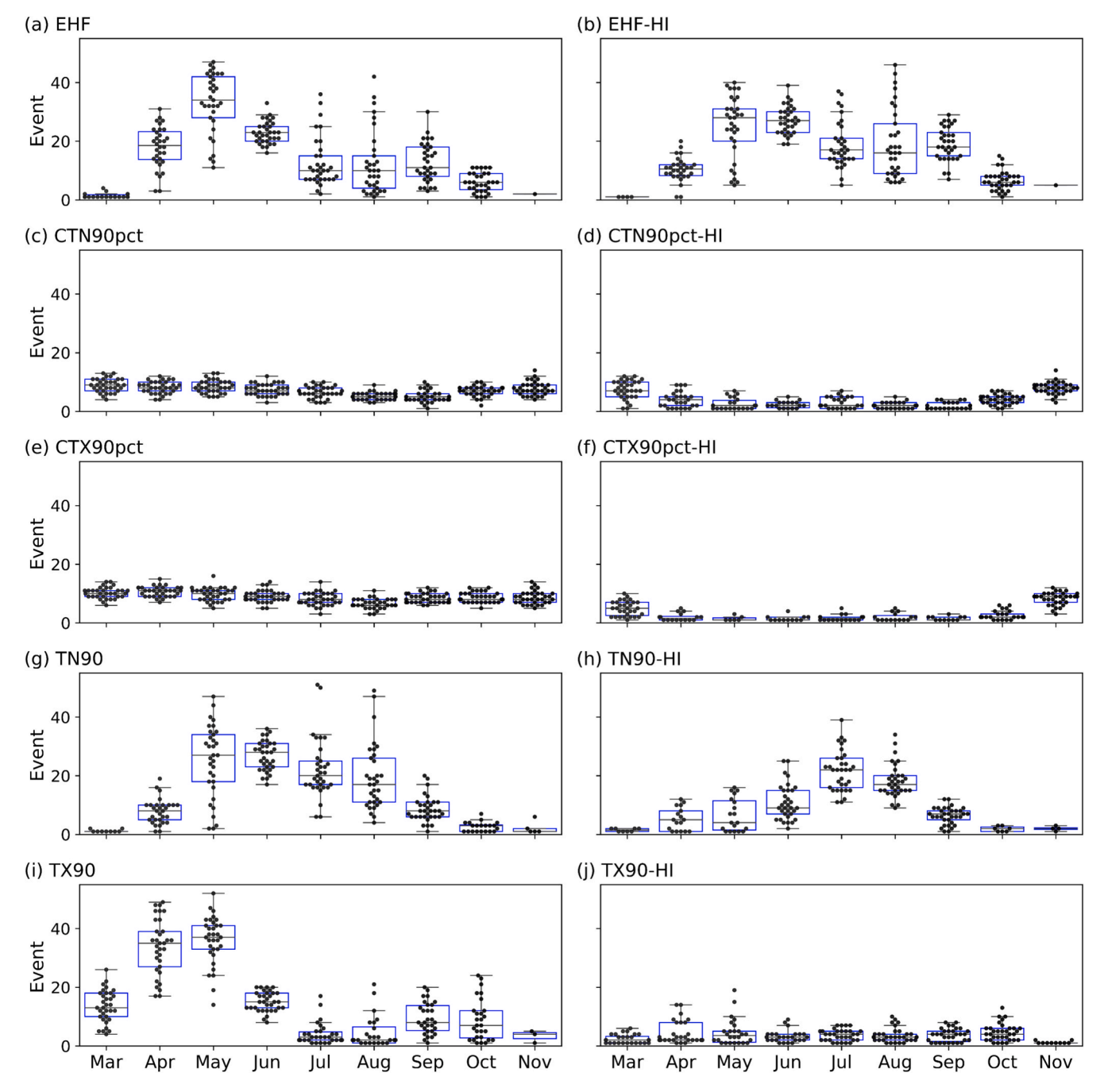


Fig. 4. Total number of HW events. Each dot represents the total HW events observed at each weather station, 1993-2022.

When analyzing the average monthly duration of HWs across Bangladesh, April exhibited the highest annual average duration for  $T_{\rm air}$ -based indices (Supplementary Fig. S2(a)). For instance, the TN90-HI index also indicated the longest HW duration in April, with an average of 4.88 days per year, coinciding with relatively low average RH of 75.79 % (Supplementary Fig. S2(b-c)). HI-based indices, however, displayed the longest HW durations in different months: May (6.30 days/year) for EHF-HI and November (4.52 and 3.70 days/year) for CTN90pct-HI and CTX90pct-HI, respectively. As humidity increased during the later part of summer, when  $T_{\rm air}$  remained high and the diurnal temperature range (DTR) narrowed (Supplementary Fig. S2(c)), fluctuations in  $T_{\rm air}$  were found to influence DTR.

A seasonal shift in the percentage of HW events was observed when humidity was considered (Fig. 6). Using climatological thresholds, daytime HWs (TX90) were more prevalent (68.39 %) during the pre-

monsoon season, whereas nocturnal HWs were predominantly recorded during the monsoon (TN90  $69.18\,\%$  and TN90-HI  $88.39\,\%$ ). A more balanced distribution of HW events between the pre-monsoon and monsoon seasons was observed for EHF, CTN90pct, and CTX90pct indices. In contrast, HI-based indices exhibited a greater disparity in HW events between the two seasons.

# 3.1.2. Interannual changes in HW metrics and trend assessment

Fig. 7 illustrates interannual changes in HW metrics, highlighting some differences in HWN for  $T_{\rm air}$ -based indices. HI-based indices, except for EHF-HI, showed notable deviations from their  $T_{\rm air}$ -based counterparts. Both EHF and EHF-HI demonstrated similar patterns in terms of frequency (HWN), duration (HWD), and frequency-weighted duration (HWF). When seasonality was accounted for, nocturnal HI-based frequency (CTN90pct-HI) exhibited greater interannual fluctuations

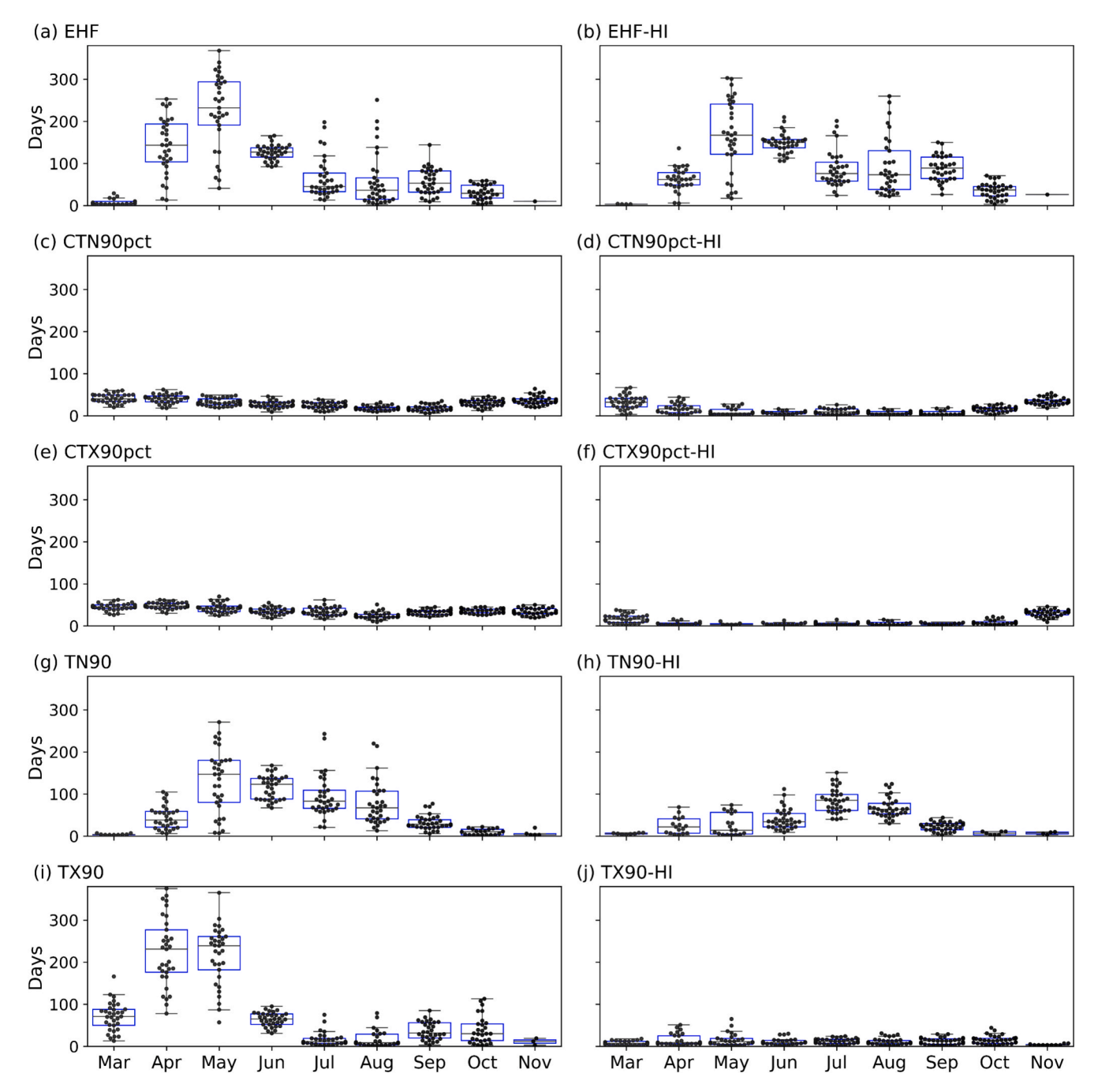


Fig. 5. Total HW days at each weather station. Each dot represents the total HW days observed.

compared to daytime HWs, a trend that also persisted in the duration metrics for nocturnal HWs. HI-based indices, excluding TX90-HI, displayed similar but more pronounced fluctuations in HW intensity metrics compared to their  $T_{\rm air}$ -based counterparts (Fig. 7(d-e)). The linear trend in HWT (Fig. 7(f)) suggested an earlier onset of HW events in recent years across most indices. However, the linear trends for CTX90pct-HI indicated a delayed onset of HWs.

The Mann-Kendall test revealed a significant increasing trend in HWN across all indices, except for CTN90pct-HI, CTX90pct-HI, and TN90-HI (Table 3). For HW duration, indices such as CTN90pct, CTN90pct-HI, CTX90pct-HI, and TN90-HI showed no statistically significant trends. Similarly, no statistically significant trends were observed in intensity metrics or onset timing, except for the average intensity (HWM) derived from the EHF index.

## 3.2. Spatial distribution and HW trends

Fig. 8 illustrates the spatial distribution of HW metrics derived from EHF. The HWN and HWD metrics display contrasting patterns across the country (Fig. 8(a-b)). The northeast region experienced a higher frequency of HW events, while longer durations were observed in the southwest. Similar spatial distributions were noted for HWN in both  $T_{\rm air}$ -based and their HI-based HW indices (Fig. 8; Supplementary Fig. S3-S11), although the HI-based indices exhibited more pronounced clustering. The HWD (longest duration) patterns for 24-hour HWs derived from both  $T_{\rm air}$ - and HI-based indices were comparable, but notable differences emerged for daytime and nocturnal HWs. A consistent increase in HW duration (HWD, HWF) was evident from the northeast to southwest, including coastal stations, for daytime HWs (Supplementary Figs. S6 and S10). In contrast, HI-based nocturnal HWs (CTN90pct-HI,

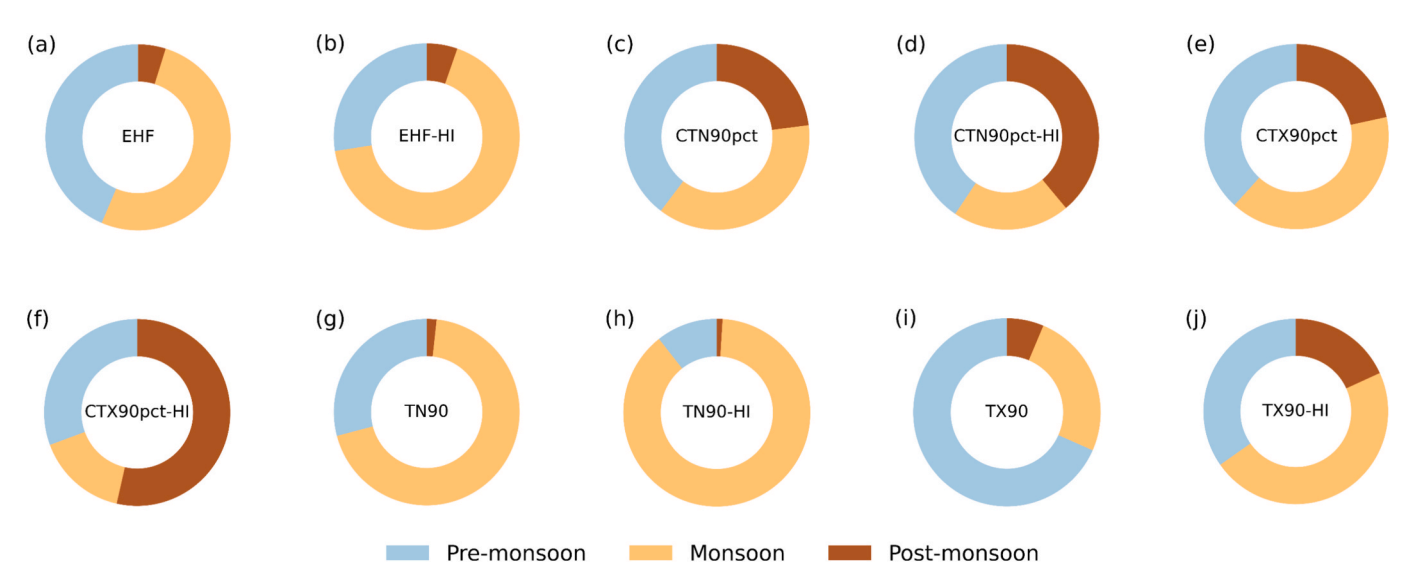


Fig. 6. Seasonal distribution of HW events, expressed as percentages of the total annual count. The figure also illustrates the influence of humidity on seasonal shifts in HW occurrence.

TN90-HI) displayed opposing spatial patterns, while  $T_{\rm air}$ -based nocturnal HWs showed extended durations in coastal stations (Supplementary Figs. S5–S6 and S9–S10).

Metrics for intensity (HWM and HWA) were consistently higher in the western regions for both EHF and EHF-HI, especially at stations like Rajshahi, Ishurdi, and Chuadanga (Fig. 8 and Supplementary Fig. S3). A similar pattern emerged for daytime HWs (CTX90pct, CTX90pct-HI, TX90), except for TX90-HI. Among the 33 stations analyzed, Hatiya and Sylhet recorded the highest intensity magnitudes (1.56 °C and 1.41 °C) and amplitudes (2.46 °C and 2.17 °C, respectively). Coastal stations generally had lower HW onset (HWT) values compared to inland stations for all indices except CTX90pct-HI (Supplementary Fig. S7(f)). This north–south distinction was most pronounced in nocturnal HWs derived from TN90 (Supplementary Fig. S8(f)).

A significant upward trend in HW frequency (HWN) and duration (HWD, HWF) was observed across many stations (Fig. 9 and Supplementary Figs. S12-S20).  $T_{\rm air}$ -based daytime HWs that accounted for seasonality showed significantly increasing trends in frequency and duration at many stations, surpassing trends observed for nocturnal HWs (Supplementary Figs. S13(a-c) and S15(a-c)). Contrasting patterns were observed when using climatological percentile thresholds (Supplementary Figs. S17 and S19). Increasing intensity trends (HWM and HWA) for daytime HWs (CTX90pct, TX90) were primarily noted in coastal and northeastern stations, notably Sylhet and Srimangal (Supplementary Figs. S15(d-e) and S19(d-e)). Meanwhile, nocturnal HWs (CTN90pct, TN90) exhibited either no trend or decreasing trends in most coastal stations (Supplementary Figs. S13(d-e) and S17(d-e)).

HI-based HW indices, apart from EHF-HI, showed limited trends in frequency and duration at most stations. The onset (HWT) of HWs clustered in coastal regions for all indices except EHF-HI, CTN90pct-HI, and CTX90pct-HI. Since HI-based indices incorporated RH, the onset of HW events was associated with rising humidity levels, typically occurring towards the end of the summer season (Supplementary Fig. S2(c)). Increasing trends indicated a delayed onset for both  $T_{\rm air}$  and HI-based indices. More stations exhibited increasing trends in HWT derived from HI-based nocturnal HWs (Supplementary Figs. S14(f) and S18(f)), suggesting delayed onsets driven by higher RH and drier summers in recent years (Supplementary Figs. S13(f) and S17(f)).

# 3.3. Comparison with ERA5 reanalysis product

The HW metrics derived from ERA5 data exhibited spatial patterns similar to those obtained from station-based observations (Fig. 10).

Additionally, the spatial distribution of trends and slopes showed a strong resemblance between the two datasets (Supplementary Fig. S21).

When comparing annual average metrics and their trends, HW intensity (HWM and HWA) demonstrated high consistency between ERA5 reanalysis and observational data (Fig. 11). Other metrics displayed similar linear trends, except for HW onset (HWT). In the ERA5 dataset, HWT showed an increasing trend, indicating a tendency for the first HW event to occur later in the year.

Pearson's correlation analysis revealed statistically significant correlation coefficients exceeding 0.5 for all metrics (Fig. 12). Notably, the  $\rm EHI_{accl}$  metric exhibited a declining trend, which can be attributed to the limited temperature variability observed over short periods or seasons (Supplementary Fig. S22). EHF-based measures similarly indicated a decline in spatial variability of temperature across stations (Supplementary Fig. S23(a)) and a reduction in temporal variability of both DTR and average  $T_{\rm air}$  during HW events (Supplementary Fig. S23 (b)). Lower  $\rm EHI_{accl}$  scores, coupled with rising HWN, HWD, and HWF, point to an ongoing shift toward prolonged warmer seasons, a trend that heightens heat stress risks for both human health and environmental systems.

# 4. Discussion

HWs are among the most destructive natural hazards globally. However, characterizing their impacts remains challenging due to the absence of a universally accepted definition (Jyoteeshkumar reddy et al., 2021; Marx et al., 2021; Tong et al., 2015). This study analyzed HW frequency, duration, intensity, and onset across Bangladesh, focusing on spatiotemporal distribution and trends using a range of indices. Five HW indices were employed to capture 24-hour (EHF), daytime (CTX90pct, TX90), and nocturnal (CTN90pct, TN90) heatwave patterns. Observational data from weather stations were compared against estimates derived from ERA5 reanalysis data. Results indicate that the 90<sup>th</sup> percentile of daily temperature serves as a reliable operational threshold for HW characterization in Bangladesh.

Due to the subtropical climate and low temperature variability in Bangladesh, higher thresholds—such as the 95<sup>th</sup> percentile—fail to effectively capture HW events. For instance, HW duration (HWD) from TX90-HI at the 95<sup>th</sup> percentile yielded comparable results to Nissan et al. (2017), yet produced too few measurable events for HW frequency and duration (Fig. 3 (a–c); Supplementary Fig. S1). Similar conclusions were drawn by Perkins and Alexander (2013) in Australia, who favored 90<sup>th</sup> percentile threshold for CTX90pct and CTN90pct. Prior research

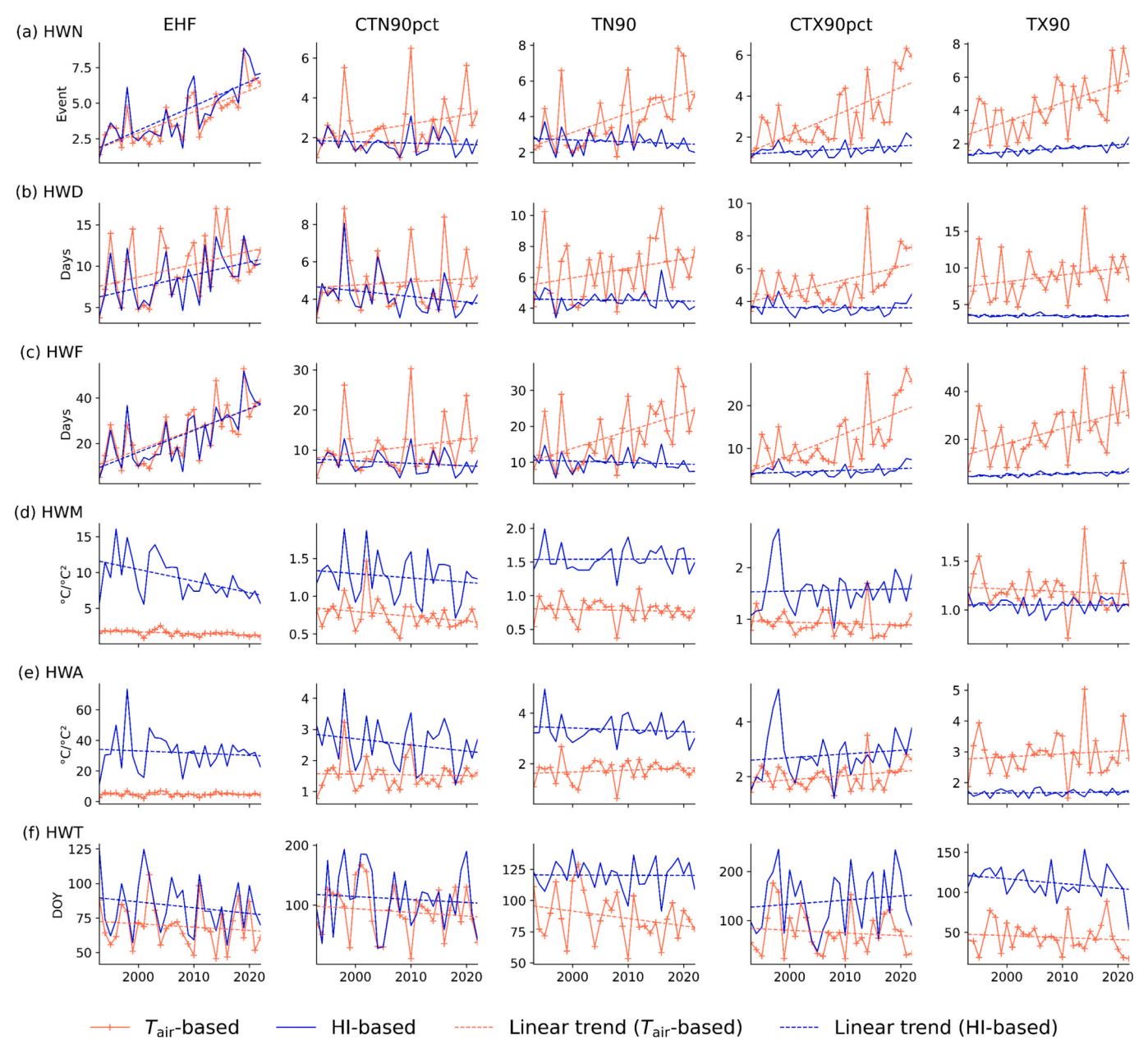


Fig. 7. Interannual changes of HW metrics. Large  $EHI_{sig}$  and  $EHI_{accl}$  resulted in a larger amplification in HWA for EHF-HI.

**Table 3**Trend of HW metrics at the annual scale.

Metric	EHF	EHF-HI	CTN90pct	CTN90pct-HI	CTX90-pct	CTX90pct-HI	TN90	TN90-HI	TX90	ТХ90-НІ
HWN	0.152*	0.176*	0.045*	-0.012	0.099*	0.012	0.106*	-0.017	0.109*	0.022*
HWD	0.187*	0.166*	0.018	-0.021	0.062*	0.001	0.07	-0.013	0.117	-0.002
HWF	0.882*	1.053*	0.126	-0.072	0.402*	0.036	0.51*	-0.071	0.576*	0.062*
HWM	-0.022*	-0.173*	-0.005	-0.006	-0.004	0.008	-0.002	0.002	-0.004	0.0003
HWA	-0.013	-0.113	0.004	-0.021	0.011	0.029	0.004	0.001	0.004	0.001
HWT	-0.371	-0.321	-0.699	-0.571	-0.234	0.809	-0.608	0.019	-0.461	-0.509

<sup>\*</sup>significant at  $p \leq 0.05$ .

underscores the need for region-specific HW thresholds (Piticar et al., 2018; Hulley, Dousset and Kahn, 2020; Mohammad and Weng, 2024). Thresholds below the 90<sup>th</sup> percentile, such as the 85<sup>th</sup>, tend to overestimate HW occurrences, reinforcing the 90<sup>th</sup> percentile as a balanced and suitable choice—consistent with findings in the One Belt One Road region (Yin, et al., 2020).

Most HWs were observed during the summer and monsoon seasons, with a higher concentration in summer for indices such as CTN90pct, CTN90pct-HI, and CTX90pct-HI (Fig. 6). This aligns with higher variability in  $T_{\rm air}$  and RH during these periods (Supplementary Fig. S2; Table S1). April, marked by peak  $T_{\rm max}$  (Supplementary Fig. S2(c)), recorded the longest HW durations, consistent with Zachariah et al.

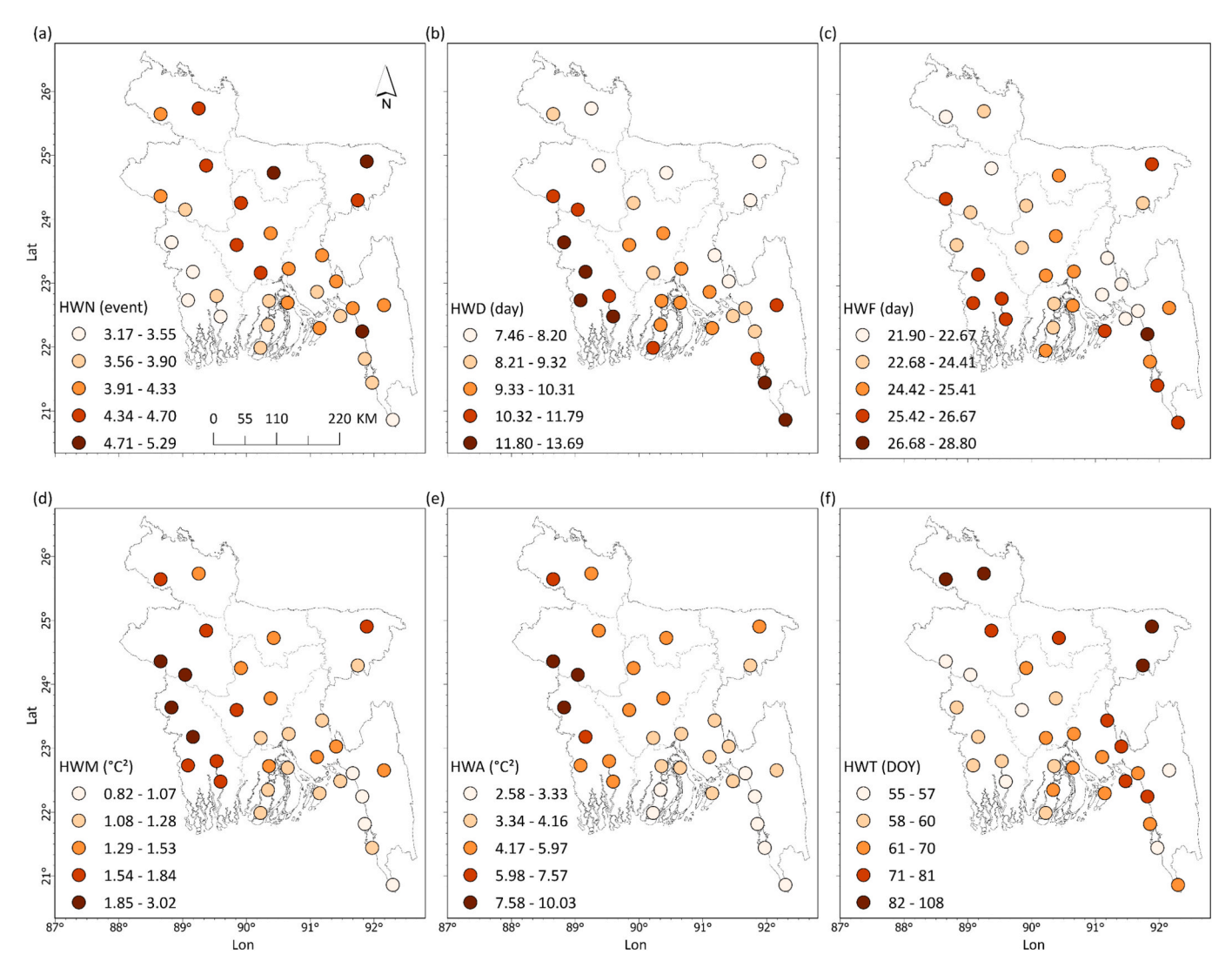


Fig. 8. Spatial distribution of the HW metrics: (a) HWN, (b) HWD, (c) HWF, (d) HWM, (e) HWA, (f) HWT, using EHF at 90<sup>th</sup> percentile.

(2023). Indices that incorporate seasonality (CTX90pct, CTN90pct, and their HI-based variants) were more responsive to changes in  $T_{\rm air}$  and RH, as well as DTR. In contrast, the monsoon season—with lower intraseasonal  $T_{\rm air}$  and RH variability (Supplementary Fig. S2; Table S1)—exhibited fewer HW events (Fig. 4) and days (Fig. 5). Similarly, EHF-based indices, which account for prior temperature anomalies, were less sensitive to short-term variability and reflected broader seasonal  $T_{\rm max}$  trends (Supplementary Fig. S2(c)).

Daytime and nocturnal HWs showed distinct temporal patterns. March and November, which typically experience cooler nights (lower  $T_{\min}$ ), showed limited variability in TN90-based HW events (Fig. 4(g); Fig. 5(g)). This effect extended to EHF and EHF-HI indices, which also demonstrated lower variability. Daytime HWs (TX90) were concentrated in summer, consistent with Nissan et al. (2017), while nocturnal HWs were moderately distributed during monsoon months (Fig. 4(g-h); Fig. 5(g-h)). This suggests that although nights in the monsoon season are warmer than in other periods, they still provide some relief after hot days. However, the persistence of high humidity at night, particularly in monsoon months, can impair nighttime recovery and reduce productivity (Adnan et al., 2024).

The comparison between  $T_{\rm air}$ -based and HI-based indices revealed important distinctions. While EHF-HI closely mirrored  $T_{\rm air}$ -based EHF in terms of frequency (HWN) and duration (HWD, HDF), other HI-based indices (CTN90pct-HI, CTX90pct-HI) showed lower variability and

displayed declining trends, suggesting reduced atmospheric moisture in recent years (Imran et al., 2023). For example, HWN from CTN90pct-HI showed less interannual fluctuation and a downward trend, in contrast to the upward trend observed in CTN90pct. These differences likely stem from variations in RH within the 15-day seasonal windows used in these indices. Moreover, recent studies indicate a positive association between daytime HWs and increased land moisture outflows (Wu et al., 2023).

Spatial differences in HW trends and intensities were also evident (Fig. 8). Inland areas showed variability between eastern and western zones, potentially due to the presence of wetlands, river networks, higher rainfall, and the small hills of northeastern Bangladesh-factors that can moderate HW impacts and lead to shorter, more frequent events (Adnan et al., 2024). Coastal areas experienced longer HW durations, suggesting sea surface temperatures (SSTs) may play a role (Raja et al., 2021). Coastal Bangladesh is generally warmer—especially in winter--compared to inland regions (Abdullah et al., 2022). Higher HW frequency and duration in coastal regions, particularly for nocturnal and daytime HWs (e.g., CTN90pct, TN90, TX90), suggest coastal proximity amplifies nocturnal HW events. A similar trend was observed for HW onset (HWT), which occurred earlier in coastal areas than inland, based on both observation (Fig. 8(f) and Fig. 9(f)) and ERA5 data (Fig. 10(f) and Supplementary Fig. S21(f)). One likely explanation is the warming influence of SSTs in contrast with the cooler inland winds during the winter-to-summer transition (Rahman et al., 2024). Further

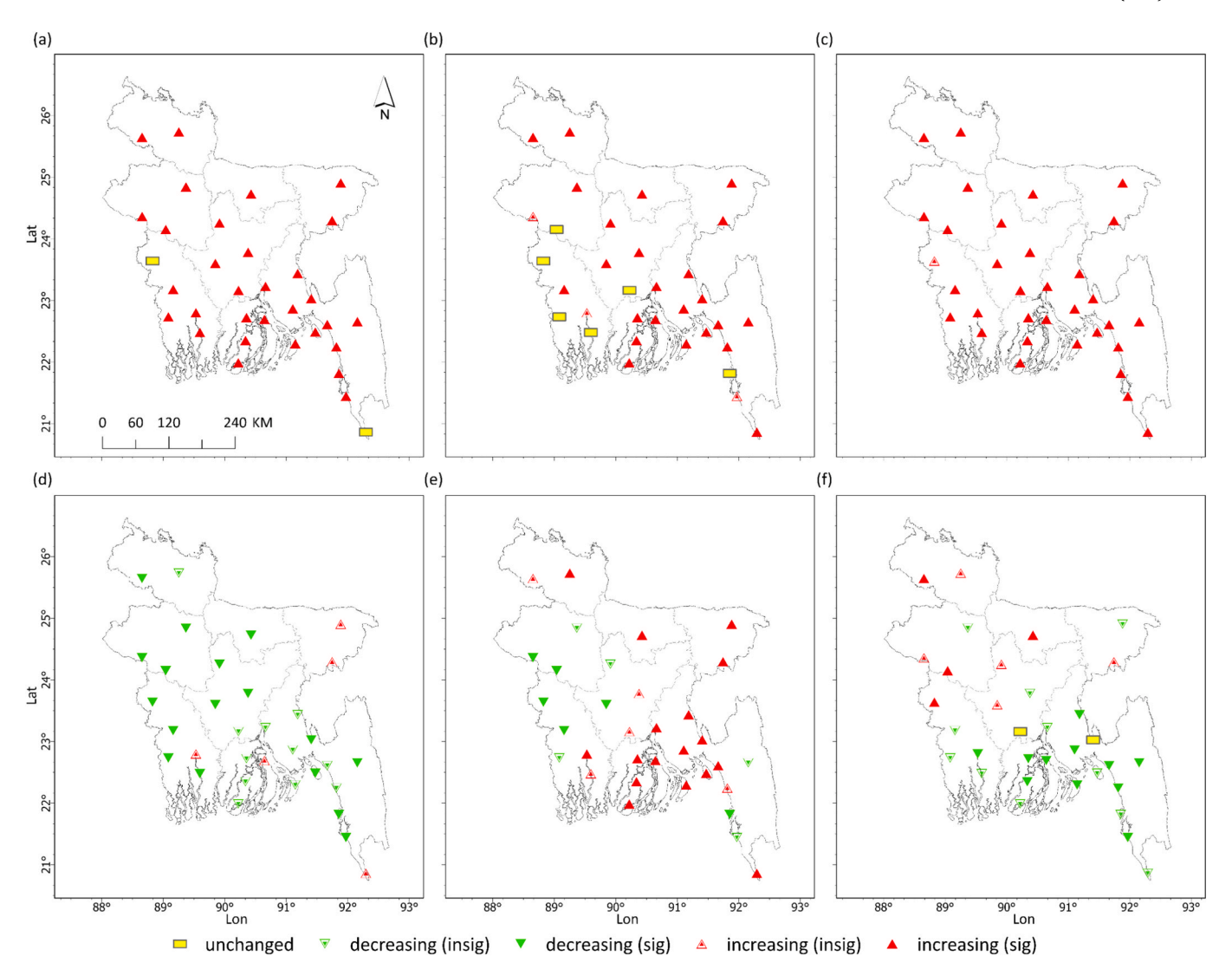


Fig. 9. EHF-derived trends: (a) HWN, (b) HWD, (c) HWF, (d) HWM, (e) HWA, (f) HWT.

investigation into local and regional atmospheric circulation is warranted. For example, Luo et al. (2025) and Wu et al. (2023) reported that daytime HWs are associated with reduced cloud cover, while nocturnal HWs correlate with increased cloud cover. The former enhances solar radiation and reduces humidity, while the latter increases longwave radiation, intensifying nighttime warming.

Expected discrepancies in HW measures across indices reflect differences in their mathematical structures, input variables, and threshold criteria. Metrics using maximum, minimum, or mean temperatures-along with differing durations and baselines-led to varied HW characterizations. These differences produced some surprising results, such as declining trends in HW intensity, particularly HWM (Fig. 6 & Table 3). This is consistent with Perkins and Alexander (2013), who reported similar trends in tropical northern Australia and attributed them to low seasonal variability in temperature. These findings reinforce the importance of using multiple indices to ensure a comprehensive understanding of HW behavior. Each index captured unique dimensions of HWs, and their combined use helped elucidate broader spatial and temporal patterns, Among them, EHF, TN90, TX90, and their HI-based variants were most effective, while CTX90pct and CTN90pct (and their HI versions) underperformed during the monsoon season, likely due to limited seasonal temperature variability in the region.

The reliability of HW measures also depends on the quality and spatial coverage of weather stations. Geographic variations in HW

characteristics are influenced by topography, surface processes, and human activities. The uneven distribution of stations in Bangladesh may have introduced some bias. Future studies should consider using continuous surface datasets, such as satellite-based products, to overcome these limitations. Additionally, using daily average RH with  $T_{\rm max}$  and  $T_{\rm min}$  to calculate HI may underestimate HI-based HWs. Incorporating daily maximum and minimum RH would likely improve accuracy. Moreover, the HI metric does not account for indoor heat stress, which poses significant risks, especially in densely built urban environments with poor ventilation. Future research should integrate indoor temperature records and HW event timestamps to assess indoor exposure and its health implications. These insights would support the development of targeted adaptation strategies for vulnerable populations.

Recent studies have also highlighted the increasing frequency and severity of compound heatwaves—events characterized by concurrent extreme daytime and nighttime temperatures over multiple days (Wang et al., 2020; Zhang et al., 2022; Wu et al., 2023; Luo et al., 2025). Such events are particularly dangerous due to the lack of nocturnal cooling, which prevents physiological recovery and elevates health risks. Although the present study examined daytime and nocturnal HWs separately, it did not incorporate compound HW metrics into the analysis. Future research should explicitly identify and assess compound HWs using integrated metrics that capture both  $T_{\rm max}$  and  $T_{\rm min}$  extremes within the same diurnal cycle. This would provide a more holistic

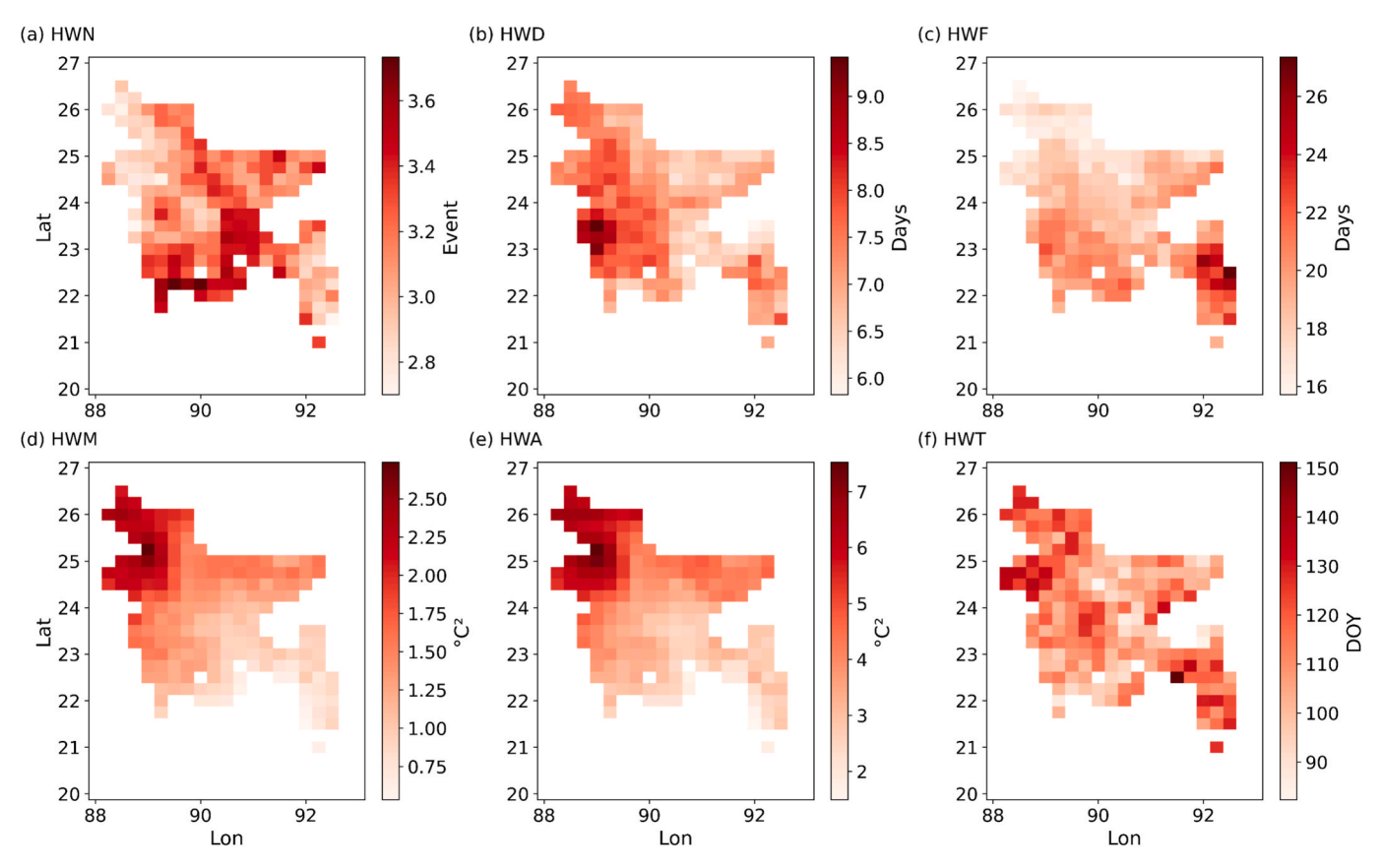


Fig. 10. Average HW metrics derived from EHF over 30 years using ERA5 data.

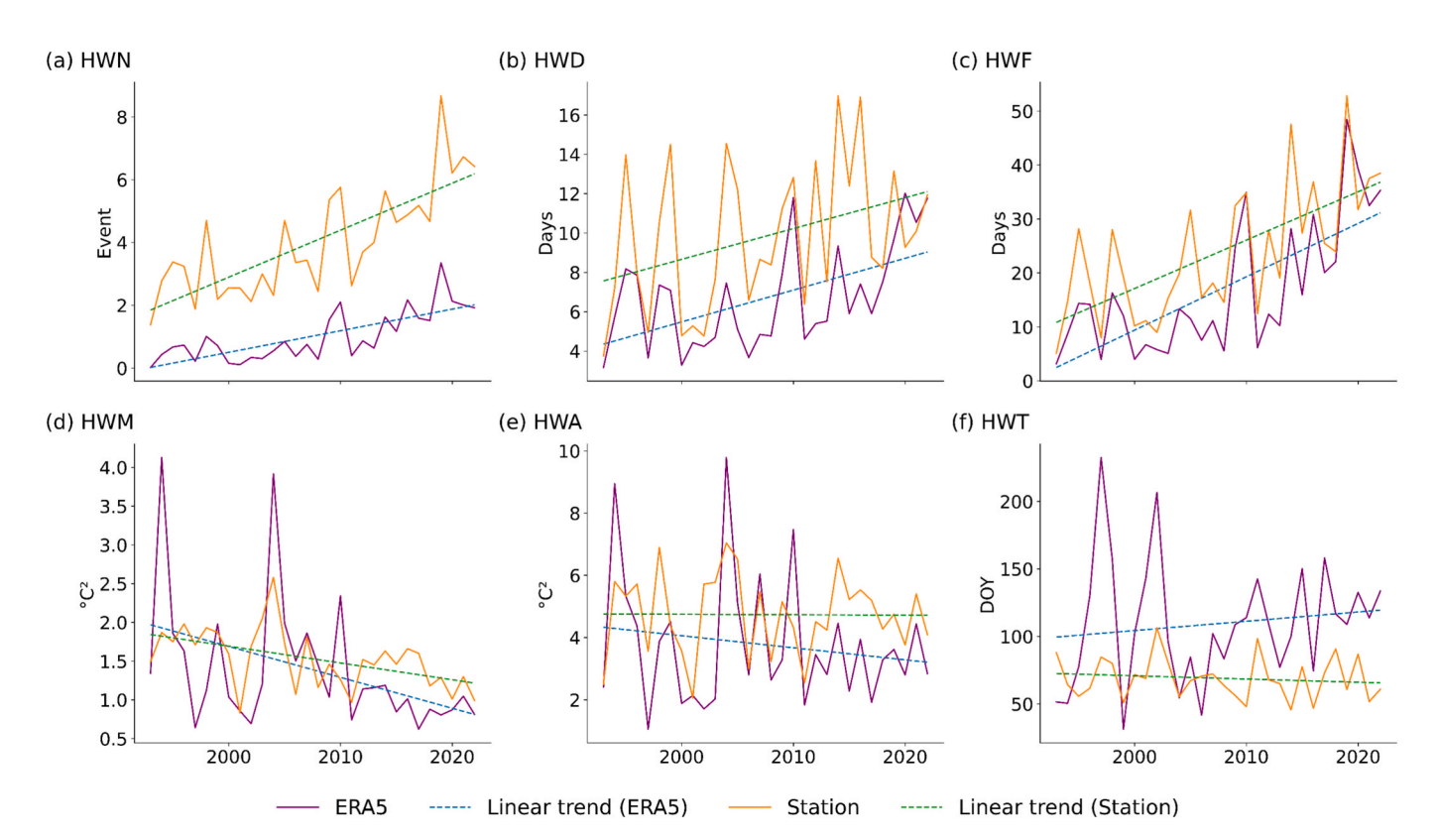


Fig. 11. Interannual changes of average HW metrics from ERA5 and observed data. The metrics are calculated using EHF.

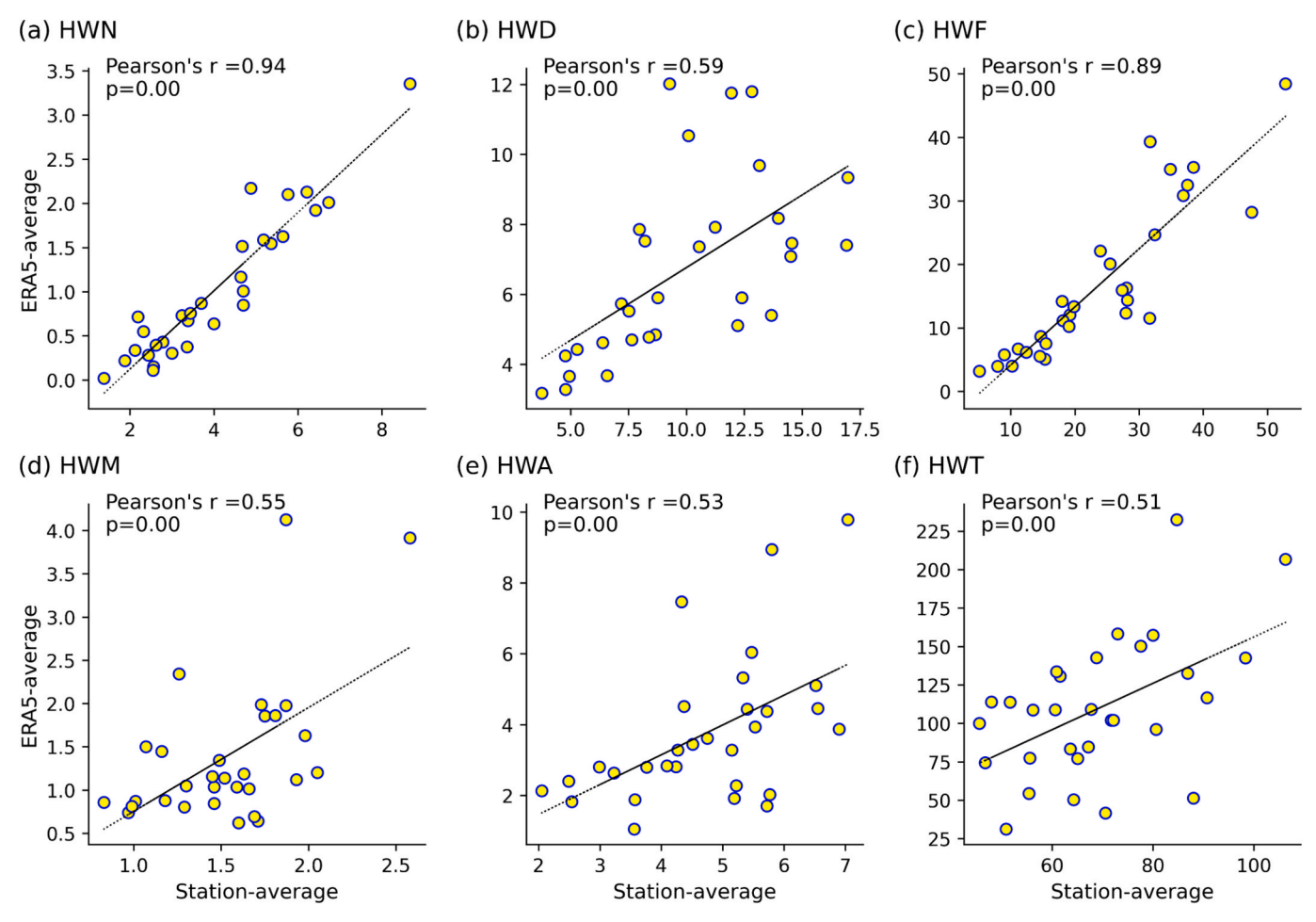


Fig. 12. Correlation between interannual ERA5-averaged HW metrics and station-averaged metrics.

understanding of HW impacts in Bangladesh's subtropical context, especially given rising humidity and nighttime temperatures. Additionally, investigating the atmospheric and land-surface drivers of compound HWs could yield valuable insights into their formation and persistence.

# 5. Conclusion

This study applied five heatwave (HW) indices—covering 24-hour (EHF), daytime (CTX90pct, TX90), and nocturnal (CTN90pct, TN90) events—to analyze HW frequency, duration, intensity, and onset across Bangladesh using both ambient and apparent temperature data. The 90<sup>th</sup> percentile emerged as the most suitable threshold for HW characterization in the country. However, EHF-based intensity values should be interpreted cautiously, as persistently high baseline temperatures can yield low magnitude estimates. Across indices, declining intensity trends and reduced temperature variability at both national and station scales point to a warmer, more stable, and uniform thermal regime. Simultaneously, the consistent advancement in HW onset dates signals an alarming shift toward earlier extreme heat events. Rising trends in HW frequency and duration underscore the urgency of implementing effective heat-risk mitigation measures.

Spatiotemporal analyses revealed that April consistently experienced the longest HW durations, while summer recorded the highest frequency and persistence of events. Coastal and inland areas, as well as eastern and western regions, displayed distinct HW characteristics, reflecting the influence of geography, climate variability, and local environmental factors. The increasing prevalence of both daytime and nocturnal HWs—coupled with shorter recovery periods between

events—amplifies risks to human health, productivity, and overall resilience.

In summary, HWs in Bangladesh are becoming more frequent, longer lasting, and occurring earlier in the year, with pronounced regional disparities in their manifestation. These trends present significant public health and socioeconomic challenges. Future research should integrate high-resolution continuous datasets, such as satellite-based observations, and account for indoor heat stress to better capture the full spectrum of HW impacts. Such efforts will provide critical evidence to inform targeted interventions, strengthen early warning systems, and build climate resilience in vulnerable communities.

# CRediT authorship contribution statement

Salit Chakma: Writing – review & editing, Writing – original draft, Visualization, Software, Methodology, Formal analysis, Data curation, Conceptualization. Abu Yousuf Md Abdullah: Writing – review & editing, Writing – original draft, Validation, Resources, Investigation, Conceptualization. Mohammed Sarfaraz Gani Adnan: Writing – review & editing, Writing – original draft, Resources, Investigation, Funding acquisition, Conceptualization. Md Saqib Shahriar: Writing – review & editing, Visualization, Software, Resources, Data curation. Mohammad Al Masum Molla: Writing – review & editing, Visualization, Resources, Investigation, Conceptualization. Ashraf Dewan: Writing – review & editing, Validation, Supervision, Resources, Methodology, Investigation, Conceptualization.

#### Declaration of competing interest

The authors declare that they have no known competing financial interests or personal relationships that could have appeared to influence the work reported in this paper.

# Acknowledgement

Mohammed Sarfaraz Gani Adnan acknowledges support from the Leverhulme Trust through an Early Career Fellowship [grant reference ECF-2023-074].

# Appendix A. Supplementary data

Supplementary data to this article can be found online at https://doi.org/10.1016/j.cliser.2025.100609.

## Data availability

Data will be made available on request.

#### References

- Abdullah, A.Y.M. et al. (2022) 'Extreme temperature and rainfall events in Bangladesh: A comparison between coastal and inland areas', International Journal of Climatology, 42(6), pp. 3253–3273. Available at: doi: 10.1002/joc.6911.
- Adhikary, T.S. (2024) 'Road Surface Melting: Bargain bitumen failing to bear extreme heat', The Daily Star, 28 April. Available at: https://www.thedailystar.net/news/bangladesh/transport/news/road-surface-melting-bargain-bitumen-failing-bear-extreme-heat-3596901 (Accessed: 25 July 2024).
- Adnan, M.S.G. et al. (2024) 'Heatwave vulnerability of large metropolitans in Bangladesh: An evaluation', Geomatica, 76(2), p. 100020. Available at: doi: 10.1016/j.geomat.2024.100020.
- Alexander, L.V. et al. (2006) 'Global observed changes in daily climate extremes of temperature and precipitation', Journal of Geophysical Research: Atmospheres, 111 (D5), p. 2005JD006290. Available at: doi: 10.1029/2005JD006290.
- Bangladesh Red Crescent Society (2021) Feasibility Study on Heatwave in Dhaka. Dhaka, Bangladesh: Bangladesh Red Crescent Society. Available at: https://bdrcs.org/wp-content/uploads/2021/09/Heat-Wave-Feasibility-Study-Final-publish-version-07-September-2021.pdf (Accessed: 26 July 2024).
- Bardhan, M. et al. (2024) 'Estimating economic losses from perceived heat stress in a global south country, Bangladesh', Urban Climate, 56, p. 102072. Available at: doi: 10.1016/j.uclim.2024.102072.
- Barriopedro, D. et al. (2023) 'Heat Waves: Physical Understanding and Scientific Challenges', Reviews of Geophysics, 61(2), p. e2022RG000780. Available at: doi: 10.1029/2022RG000780.
- van Buuren, S. (2018) Flexible Imputation of Missing Data, Second Edition. 2nd edn. Second edition. | Boca Raton, Florida: CRC Press, [2019] |: Chapman and Hall/CRC Available at: doi: 10.1201/9780429492259.
- Choi, Y.-W. et al. (2021) 'Near-term regional climate change over Bangladesh', Climate Dynamics, 57(11–12), pp. 3055–3073. Available at: doi: 10.1007/s00382-021-05856-2
- Chowdhury, A.R. (2024) 'Heatwave: Inside the boiling pot of inequality', The Daily Star, 18 April. Available at: https://www.thedailystar.net/opinion/views/news/heatwave-inside-the-boiling-pot-inequality-3299996 (Accessed: 25 July 2024).
- Copernicus Climate Data Store (2018) ERA5 hourly data on single levels from 1940 to present, Copernicus Climate Data Store. Available at: https://cds.climate.copernicus.eu/cdsapp#!/dataset/reanalysis-era5-single-levels?tab=form.
- CRED and UNDRR (2020) The human cost of disasters: An overview of the last 20 years (2000-2019). Centre for Research on the Epidemiology of Disasters (CRED); United Nations Office for Disaster Risk Reduction, p. 30. Available at: https://www.undrr.org/publication/human-cost-disasters-overview-last-20-years-2000-2019.
- Dewan, A., Kiselev, G. and Botje, D. (2021) 'Diurnal and seasonal trends and associated determinants of surface urban heat islands in large Bangladesh cities', Applied Geography, 135, p. 102533. Available at: doi: 10.1016/j.apgeog.2021.102533.
- Dong, Z. et al. (2021) 'Heatwaves in Southeast Asia and Their Changes in a Warmer World', Earth's Future, 9(7), p. e2021EF001992. Available at: doi: 10.1029/ 2021EF001992.
- Ebi, K.L. et al. (2021) 'Hot weather and heat extremes: health risks', The Lancet, 398 (10301), pp. 698–708. Available at: doi: 10.1016/S0140-6736(21)01208-3.
- Ehsan, M.A. et al. (2023) 'The ENSO Fingerprint on Bangladesh Summer Monsoon Rainfall', Earth Systems and Environment, 7(3), pp. 617–627. Available at: doi: 10.1007/s41748-023-00347-z.
- Fischer, E.M. and Schär, C. (2010) 'Consistent geographical patterns of changes in highimpact European heatwaves', Nature Geoscience, 3(6), pp. 398–403. Available at: doi: 10.1038/ngeo866.
- García-León, D. et al. (2021) 'Current and projected regional economic impacts of heatwaves in Europe', Nature Communications, 12(1), p. 5807. Available at: doi: 10.1038/s41467-021-26050-z.

Guo, Q. et al. (2024) 'Regional variation in the role of humidity on city-level heat-related mortality', PNAS Nexus. Edited by J. Zhang, 3(8), p. pgae290. Available at: doi: 10.1093/pnasnexus/pgae290.

- Habeeb, D., Vargo, J. and Stone, B. (2015) 'Rising heat wave trends in large US cities', Natural Hazards, 76(3), pp. 1651–1665. Available at: doi: 10.1007/s11069-014-1563-z
- Handmer, J. et al. (2012) 'Changes in Impacts of Climate Extremes: Human Systems and Ecosystems', in C.B. Field et al. (eds) Managing the Risks of Extreme Events and Disasters to Advance Climate Change Adaptation. 1st edn. Cambridge University Press, pp. 231–290. Available at: doi: 10.1017/CBO9781139177245.007.
- Hersbach, H. et al. (2020) 'The ERA5 global reanalysis', Quarterly Journal of the Royal Meteorological Society, 146(730), pp. 1999–2049. Available at: doi: 10.1002/ gi.3803.
- Hossain, E. and Manik, R.K. (2022) 'Heatwave causes 27 deaths', New Age, 16 July. Available at: https://www.newagebd.net/article/176013/heatwave-causes-27-deaths (Accessed: 26 July 2024).
- Hoyer, S. et al. (2023) 'xarray'. [object Object]. Available at: doi: 10.5281/ZENODO.8153447.
- Hulley, G.C., Dousset, B. and Kahn, B.H. (2020) 'Rising trends in heatwave metrics across southern california', Earth's Future, 8(7). Available at: doi: 10.1029/ 2020EF001480.
- Hussain, Md. and Mahmud, I. (2019) 'pyMannKendall: a python package for non parametric Mann Kendall family of trend tests.', Journal of Open Source Software, 4 (39), p. 1556. Available at: doi: 10.21105/joss.01556.
- Imran, H.M. et al. (2023) 'Spatiotemporal analysis of temperature and precipitation extremes over Bangladesh using a novel gridded observational dataset', Weather and Climate Extremes, 39, p. 100544. Available at: doi: 10.1016/j.wace.2022.100544.
- Islam, M.J. (2024) 'Bangladesh faces longest, hottest spell on record', The Business Standard, 27 April. Available at: https://www.tbsnews.net/bangladesh/ environment/bangladesh-experiencing-longest-heatwave-record-837041 (Accessed: 26 July 2024).
- Jyoteeshkumar reddy, P., Perkins-Kirkpatrick, S.E. and Sharples, J.J. (2021) 'Intensifying Australian Heatwave Trends and Their Sensitivity to Observational Data', Earth's Future, 9(4), p. e2020EF001924. Available at: doi: 10.1029/2020EF001924.
- Kagawa, F. (2022) The Heat is On! Towards Climate Resilient Education Systems in South Asia. Kathmandu: UNICEF Regional Office for South Asia. Available at:.
- Khan, M. et al. (2019) 'Observed trends in climate extremes over Bangladesh from 1981 to 2010', Climate Research, 77(1), pp. 45–61. Available at: doi: 10.3354/cr01539.
- Kornhuber, K. et al. (2024) 'Global emergence of regional heatwave hotspots outpaces climate model simulations', Proceedings of the National Academy of Sciences, 121 (49), p. e2411258121. Available at: doi: 10.1073/pnas.2411258121.
- Li, K. and Amatus, G. (2020) 'Spatiotemporal changes of heat waves and extreme temperatures in the main cities of China from 1955 to 2014', Natural Hazards and Earth System Sciences, 20(7), pp. 1889–1901. Available at: doi: 10.5194/nhess-20-1889-2020.
- Loughran, T. (2021) 'tammasloughran/ehfheatwaves: First Zenodo release'. [object Object]. Available at: doi: 10.5281/ZENODO.5637520.
- Luo, M., Lau, N.-C. and Liu, Z. (2022) 'Different mechanisms for daytime, nighttime, and compound heatwaves in southern China', Weather and Climate Extremes, 36, p. 100449. Available at: doi: 10.1016/j.wace.2022.100449.
- Luo, Y. et al. (2025) 'Distinctive local and large-scale processes associated with daytime, nighttime, and compound heatwaves in China', Weather and Climate Extremes, 47, 100749. Available at: doi: 10.1016/j.wace.2025.100749.
- Mahmud, F. (2023) 'Bangladesh suffers long power cuts amid worst heatwave in decades', Al Jazeera, 8 June. Available at: https://www.aljazeera.com/news/2023/6/8/bangladesh-suffers-long-power-cuts-amid-worst-heatwave-in-decades.
- Mahmud, I., Raza, W.A. and Hossain, M.R. (2021) Climate Afflictions. Washington DC: World Bank. Available at: https://hdl.handle.net/10986/36333.
- Majumder, A.K. (2024) 'Heatwave alert: Dhaka's scorching situation and long-term environmental destruction', The Business Standard, 22 April. Available at: https://www.tbsnews.net/thoughts/heatwave-alert-dhakas-scorching-situation-and-long-term-environmental-destruction-834161 (Accessed: 26 July 2024).
- Mann, H.B. (1945) 'Nonparametric Tests Against Trend', Econometrica, 13(3), p. 245.
  Available at: doi: 10.2307/1907187.
- Marx, Werner, Robin Haunschild, and Lutz Bornmann. 'Heat waves: a hot topic in climate change research.' Theoretical and applied climatology 146.1 (2021): 781-800. Available at: doi: 10.1007/s00704-021-03758-y.
- Miller, S. et al. (2021) 'Heat Waves, Climate Change, and Economic Output', Journal of the European Economic Association, 19(5), pp. 2658–2694. Available at: doi: 10.1093/jeea/jvab009.
- Miralles, D.G. et al. (2019) 'Land-atmospheric feedbacks during droughts and heatwaves: state of the science and current challenges', Annals of the New York Academy of Sciences, 1436(1), pp. 19–35. Available at: doi: 10.1111/nyas.13912.
- Mohammad, P. and Weng, Q. (2024) 'Comparing existing heat wave indices in identifying dangerous heat wave outdoor conditions', Nexus, p. 100027. Available at: doi: 10.1016/j.ynexs.2024.100027.
- Mustajib, S. (2024) 'Extreme Heatwaves in Bangladesh: The Environmental Governance Perspectives', The Diplomat, 25 April. Available at: https://thediplomat.com/2024/ 04/extreme-heatwaves-in-bangladesh-the-environmental-governance-perspectives/ (Accessed: 26 July 2024).
- Nabil, N. (2024) 'Bangladesh faced 57 extra days of extreme heat in last 12 months', DhakaTribune, 31 May. Available at: https://www.dhakatribune.com/bangladesh/bangladesh-environment/348005/bangladesh-faced-57-extra-days-of-extreme-heat-in (Accessed: 26 July 2024).
- Nairn, J., Fawcett, R. and Ray, D. (2009) 'Defining and predicting excessive heat events, a national system', in Modelling and understanding high impact weather: extended

- abstracts of the third CAWCR Modelling Workshop. Melbourne, Australia (30 November 2 December 2009), pp. 83–86.
- Nairn, J.R. and Fawcett, R.J.B. (2014) 'The excess heat factor: A metric for heatwave intensity and its use in classifying heatwave severity', International Journal of Environmental Research and Public Health, 12(1), pp. 227–253. Available at: doi: 10.3390/ijerph120100227.
- Nandy, D. (2024) 'First heatwave, now water crisis', The Daily Star, 1 May. Available at: https://www.thedailystar.net/news/bangladesh/news/first-heatwave-now-water-crisis-3599481 (Accessed: 26 July 2024).
- Ng, K. (2024) 'Searing heat shuts schools for 33 million children', BBC News. Online, 25 April. Available at: https://www.bbc.com/news/articles/c1wxij3g9650 (Accessed: 26 July 2024).
- Nissan, H. et al. (2017) 'Defining and predicting heat waves in Bangladesh', Journal of Applied Meteorology and Climatology, 56(10), pp. 2653–2670. Available at: doi: 10.1175/JAMC-D-17-0035.1.
- Luo, Y. et al. (2025) 'Distinctive local and large-scale processes associated with daytime, nighttime and compound heatwaves in China', Weather and Climate Extremes, 47, p. 100749. Available at: doi: 10.1016/j.wace.2025.100749.
- Oliveira, A., Lopes, A., Soares, A., 2022. 'Excess heat factor climatology, trends, and exposure across european functional urban areas', Weather and Climate Extremes, 36. Available at: https://doi.org/10.1016/j.wace.2022.100455.
- Paul, R. and Varadhan, S. (2023) 'Bangladesh suffers widespread power outages during relentless heat', Reuters, 21 April. Available at: https://www.reuters.com/world/ asia-pacific/bangladesh-suffers-widespread-power-outages-during-relentless-heat-2023-04-20/ (Accessed: 26 July 2024).
- Perkins, S.E. and Alexander, L.V. (2013) 'On the Measurement of Heat Waves', Journal of Climate, 26(13), pp. 4500–4517. Available at: doi: 10.1175/JCLI-D-12-00383.1.
- Piticar, A. et al. (2018) 'Recent changes in heat waves and cold waves detected based on excess heat factor and excess cold factor in Romania', International Journal of Climatology, 38(4), pp. 1777–1793. Available at: doi: 10.1002/joc.5295.
- Rahman, Md.M. et al. (2024) 'Are hotspots and frequencies of heat waves changing over time? Exploring causes of heat waves in a tropical country', PLOS ONE. Edited by S. Heddam, 19(5), p. e0300070. Available at: doi: 10.1371/journal.pone.0300070.
- Raja, Debasish Roy, et al. 'Spatial distribution of heatwave vulnerability in a coastal city of Bangladesh.' Environmental Challenges 4 (2021): 100122. Available at: doi: 10.1016/j.envc.2021.100122.
- Sen, P.K. (1968) 'Estimates of the Regression Coefficient Based on Kendall's Tau', Journal of the American Statistical Association, 63(324), pp. 1379–1389. Available at: doi: 10.1080/01621459.1968.10480934.
- Shetye, S.R. et al. (1996) 'Hydrography and circulation in the western Bay of Bengal during the northeast monsoon', Journal of Geophysical Research: Oceans, 101(C6), pp. 14011–14025. Available at: doi: 10.1029/95JC03307.
- Steadman, R.G. (1979) 'The assessment of sultriness. Part I: a temperature-humidity index based on human physiology and clothing science', Journal of Applied Meteorology and Climatology, 18(7), pp. 861–873. Available at: doi: 10.1175/1520-0450(1979)018
- The Economic Times (2024) 'April temperature in Bangladesh hottest on record: Forecaster', The Economic Times, 1 May. Available at: https://m.economictimes.

- com/news/international/world-news/april-temperatures-in-bangladesh-hottest-on-record-forecaster/articleshow/109750403.cms (Accessed: 26 July 2024).
- Thomas, N.P. et al. (2020) 'Mechanisms Associated with Daytime and Nighttime Heat Waves over the Contiguous United States', Journal of Applied Meteorology and Climatology, 59(11), pp. 1865–1882. Available at: doi: 10.1175/JAMC-D-20-0053 1
- Tolika, K. (2019) 'Assessing heatwaves over greece using the excess heat factor (EHF)', Climate, 7(1). Available at: doi: 10.3390/cli7010009.
- Tong, S. et al. (2015) 'Exploration of the health risk-based definition for heatwave: A multi-city study.' Environmental research, 142, 696-702. Available at: doi: 10.1016/j.envres.2015.09.009.
- Tuholske, C. et al. (2021) 'Global urban population exposure to extreme heat', Proceedings of the National Academy of Sciences, 118(41), p. e2024792118. Available at: doi: 10.1073/pnas.2024792118.
- Vogel, M.M. et al. (2019) 'Concurrent 2018 Hot Extremes Across Northern Hemisphere Due to Human-Induced Climate Change', Earth's Future, 7(7), pp. 692–703. Available at: doi: 10.1029/2019EF001189.
- Wang, J. et al., (2020) 'Anthropogenically-driven increases in the risks of summertime compound hot extremes', Nature Communications, 11, 528. Available at: doi: 10.1038/s41467-019-14233-8.
- Wu, J. et al. (2018) 'Influences of heatwave, rainfall, and tree cover on cholera in Bangladesh', Environment International, 120, pp. 304–311. Available at: doi: 10.1016/j.envint.2018.08.012.
- Wu, S. et al. (2023) 'Local mechanisms for global daytime, nighttime, and compound heatwaves', npj Climate and Atmospheric Science, 6(1), p. 36. Available at: doi: 10.1038/s41612-023-00365-8.
- Yasumoto, S. et al. (2019) 'Heat exposure assessment based on individual daily mobility patterns in Dhaka, Bangladesh', Computers, Environment and Urban Systems, 77, p. 101367. Available at: doi: 10.1016/j.compenvurbsys.2019.101367.
- Yin, C. et al. (2020) 'Spatiotemporal Distribution and Risk Assessment of Heat Waves Based on Apparent Temperature in the One Belt and One Road Region', Remote Sensing, 12(7), p. 1174. Available at: doi: 10.3390/rs12071174.
- Zachariah, M. et al. (2023) Extreme humid heat in South Asia in April 2023, largely driven by climate change, detrimental to vulnerable and disadvantaged communities. Imperial College London. Available at: doi: 10.25561/104092.
- Zhang, T. et al. (2022) 'Influences of the boreal winter Arctic Oscillation on the peaksummer compound heat waves over the Yangtze-Huaihe River basin: The North Atlantic capacitor effect'. Climate Dynamics, 59, 2331-2343. Available at: doi: 10.1007/s00382-022-06212-5.
- Zhang, X. et al. (2005) 'Avoiding Inhomogeneity in Percentile-Based Indices of Temperature Extremes', Journal of Climate, 18(11), pp. 1641–1651. Available at: doi: 10.1175/JCLI3366.1.
- Zhang, Z. (2016) 'Multiple imputation with multivariate imputation by chained equation (MICE) package', Annals of Translational Medicine, 4(2), p. 30. Available at: doi: 10.3978/j.issn.2305-5839.2015.12.63.
- Zhao, M. et al. (2021) 'Assessment of the economic impact of heat-related labor productivity loss: a systematic review', Climatic Change, 167(1–2), p. 22. Available at: doi: 10.1007/s10584-021-03160-7.